

Determination of U-Bolt Connection Load Capacities in Overhead Sign Support Structures

Final Report
June 2019



IOWA STATE UNIVERSITY
Institute for Transportation

Sponsored by
Iowa Department of Transportation
(InTrans Project 18-638)

About the Bridge Engineering Center

The mission of the Bridge Engineering Center (BEC) is to conduct research on bridge technologies to help bridge designers/owners design, build, and maintain long-lasting bridges.

About the Institute for Transportation

The mission of the Institute for Transportation (InTrans) at Iowa State University is to develop and implement innovative methods, materials, and technologies for improving transportation efficiency, safety, reliability, and sustainability while improving the learning environment of students, faculty, and staff in transportation-related fields.

Disclaimer Notice

The contents of this report reflect the views of the authors, who are responsible for the facts and the accuracy of the information presented herein. The opinions, findings and conclusions expressed in this publication are those of the authors and not necessarily those of the sponsors.

The sponsors assume no liability for the contents or use of the information contained in this document. This report does not constitute a standard, specification, or regulation.

The sponsors do not endorse products or manufacturers. Trademarks or manufacturers' names appear in this report only because they are considered essential to the objective of the document.

Iowa State University Nondiscrimination Statement

Iowa State University does not discriminate on the basis of race, color, age, ethnicity, religion, national origin, pregnancy, sexual orientation, gender identity, genetic information, sex, marital status, disability, or status as a U.S. veteran. Inquiries regarding non-discrimination policies may be directed to Office of Equal Opportunity, 3410 Beardshear Hall, 515 Morrill Road, Ames, Iowa 50011, Tel. 515-294-7612, Hotline: 515-294-1222, email eooffice@iastate.edu.

Iowa Department of Transportation Statements

Federal and state laws prohibit employment and/or public accommodation discrimination on the basis of age, color, creed, disability, gender identity, national origin, pregnancy, race, religion, sex, sexual orientation or veteran's status. If you believe you have been discriminated against, please contact the Iowa Civil Rights Commission at 800-457-4416 or Iowa Department of Transportation's affirmative action officer. If you need accommodations because of a disability to access the Iowa Department of Transportation's services, contact the agency's affirmative action officer at 800-262-0003.

The preparation of this report was financed in part through funds provided by the Iowa Department of Transportation through its "Second Revised Agreement for the Management of Research Conducted by Iowa State University for the Iowa Department of Transportation" and its amendments.

The opinions, findings, and conclusions expressed in this publication are those of the authors and not necessarily those of the Iowa Department of Transportation.

Technical Report Documentation Page

1. Report No. InTrans Project 18-638	2. Government Accession No.	3. Recipient's Catalog No.	
4. Title and Subtitle Determination of U-Bolt Connection Load Capacities in Overhead Sign Support Structures		5. Report Date June 2019	
		6. Performing Organization Code	
7. Author(s) Brent M. Phares (orcid.org/0000-0001-5894-4774) and Zhengyu Liu (orcid.org/0000-0002-7407-0912)		8. Performing Organization Report No. InTrans Project 18-638	
9. Performing Organization Name and Address Bridge Engineering Center Iowa State University 2711 South Loop Drive, Suite 4700 Ames, IA 50010-8664		10. Work Unit No. (TRAIS)	
		11. Contract or Grant No.	
12. Sponsoring Organization Name and Address Iowa Department of Transportation 800 Lincoln Way Ames, IA 50010		13. Type of Report and Period Covered Final Report	
		14. Sponsoring Agency Code	
15. Supplementary Notes Visit www.intrans.iastate.edu for color pdfs of this and other research reports.			
16. Abstract <p>The load capacities of the U-bolt connections used in steel overhead sign trusses for the Iowa Department of Transportation (DOT) are not known because the bolts are used in ways that do not match the available manufacturer data. Although these U-bolt connections appear to have performed satisfactorily in the past, there has been a growing safety concern in recent years because of the need for overhead sign trusses to support larger signs at greater span lengths.</p> <p>The objective of this project was to develop effective and efficient methodologies to realistically estimate the capacity of the U-bolt connections specified in the actual steel overhead sign truss (SOST) design standards. To achieve this objective, a comprehensive literature search on the utilization and modeling techniques for U-bolt connections was first conducted. Three laboratory tests were then conducted on two types of specimens with loading directions of 0° and 90° for the Type-A specimen and 0° for the Type-B specimen.</p> <p>The data collected from the tests were used to calibrate the finite element model. The calibrated model was then used in a parametric study to calculate the yield and ultimate capacity of both types of specimens with various material properties and load resultant directions.</p> <p>Finally, interaction diagrams were developed with limitations for design usage to estimate the capacity of the U-bolt connections with different material types and load directions.</p>			
17. Key Words finite element modeling—highway sign trusses—interaction diagrams—overhead sign supports—parametric study—U-bolt load capacity		18. Distribution Statement No restrictions.	
19. Security Classification (of this report) Unclassified.	20. Security Classification (of this page) Unclassified.	21. No. of Pages 70	22. Price NA

DETERMINATION OF U-BOLT CONNECTION LOAD CAPACITIES IN OVERHEAD SIGN SUPPORT STRUCTURES

**Final Report
June 2019**

Principal Investigator

Brent M. Phares, Research Associate Professor
Bridge Engineering Center, Iowa State University

Research Assistant

Zhengyu Liu, Research Engineer
Bridge Engineering Center, Iowa State University

Authors

Brent M. Phares and Zhengyu Liu

Sponsored by
Iowa Department of Transportation

Preparation of this report was financed in part
through funds provided by the Iowa Department of Transportation
through its Research Management Agreement with the
Institute for Transportation
(InTrans Project 18-638)

A report from
Bridge Engineering Center
Iowa State University
2711 South Loop Drive, Suite 4700
Ames, IA 50010-8664
Phone: 515-294-8103 / Fax: 515-294-0467
www.intrans.iastate.edu

TABLE OF CONTENTS

ACKNOWLEDGMENTS	ix
EXECUTIVE SUMMARY	xi
CHAPTER 1. INTRODUCTION	1
1.1 Problem Statement	1
1.2 Background	1
1.3 Objective	2
1.4 Research Plan	2
1.5 Products	2
CHAPTER 2. LITERATURE REVIEW	3
2.1 U-bolt Connection	3
2.2 Finite Element Modeling (FEM)	5
2.3 Summary	7
CHAPTER 3. LABORATORY TESTS	8
3.1 Type-A Specimens	8
3.1.1 Specimen Description	8
3.1.2 Loading Configuration	11
3.1.3 Instrumentation	14
3.1.4 Test Results	16
3.2 Type-B Specimen	23
3.2.1 Specimen Description	23
3.2.2 Loading Configuration	25
3.2.3 Instrumentation	26
3.2.4 Test Results	26
CHAPTER 4. MODEL DEVELOPMENT AND VALIDATION	29
4.1 Model Development	29
4.1.1 Type-A Specimen	29
4.1.2 Type-B Specimen	31
4.2 Model Validation	31
4.2.1 U-Bolt Steel $f_y = 36$ ksi, $f_u = 60$ ksi	31
4.2.2 U-Bolt Steel $f_y = 70$ ksi, $f_u = 110$ ksi	32
CHAPTER 5. PARAMETRIC STUDY	45
CHAPTER 6. INTERACTION DIAGRAMS	51
CHAPTER 7. SUMMARY, CONCLUSIONS AND FUTURE RESEARCH DIRECTIONS	54
7.1 Summary	54
7.2 Conclusions	54
7.3 Future Research Directions	54
REFERENCES	56

LIST OF FIGURES

Figure 1. Finite element modeling of U-bolt assembly	3
Figure 2. FEM of U-bolted leaf spring assembly	4
Figure 3. FEM of U-bolt connection.....	4
Figure 4. FEM of bolt connection.....	5
Figure 5. Boundary conditions and contact surfaces	6
Figure 6. Small-scale FEM of bolt connection	6
Figure 7. Type-A U-bolt specimen design.....	9
Figure 8. Type-A specimens	10
Figure 9. Load configurations on Type-A connection specimens	12
Figure 10. Type-A specimen setup before testing	13
Figure 11. Instrumentation on Type-A specimen	15
Figure 12. U-bolt strain due to preload (Type-A, horizontal loading).....	16
Figure 13. Shear failure on the U-bolt shanks (Type-A, horizontal loading).....	17
Figure 14. Load vs. displacement curves (Type-A, horizontal loading)	18
Figure 15. U-bolt strain due to horizontal load (Type-A, horizontal loading)	18
Figure 16. Strain from rosette strain gage (Type-A, horizontal loading)	19
Figure 17. U-bolt strain due to preload (Type-A, vertical loading).....	20
Figure 18. Failure Model (Type-A, vertical loading)	21
Figure 19. Load vs. displacement curves (Type-A, vertical loading).....	22
Figure 20. U-bolt strain due to vertical load (Type-A, vertical loading).....	22
Figure 21. Strain from rosette strain gage (Type-A, vertical loading).....	23
Figure 22. Type-B U-bolt specimen	24
Figure 23. Type-B specimen.....	24
Figure 24. Type-B specimen: force parallel to the angel (horizontal loading).....	25
Figure 25. Type-B specimen setup before testing	25
Figure 26. Instrumentation on Type-B specimen	26
Figure 27. U-bolt strain due to preload (Type-B, horizontal loading).....	27
Figure 28. Shear failure on the U-bolt shanks (Type-B, horizontal loading).....	27
Figure 29. Load vs. displacement curves (Type-B, horizontal loading).....	28
Figure 30. U-bolt strain due to horizontal load (Type-B, horizontal loading).....	28
Figure 31. Engineering and true stress-strain data.....	30
Figure 32. FEM of Type-A specimen	31
Figure 33. FEM of Type-B specimen	31
Figure 34. Model validation with load vs. displacement curves (Type-A, vertical loading)	32
Figure 35. Stress-strain data for the U-bolt on the calibrated model	33
Figure 36. von Mises strain on the U-bolt after preload	34
Figure 37. von Mises strain on the U-bolt at ultimate stage	35
Figure 38. Model validation by U-bolt strain due to preload (Type-A, horizontal loading)	36
Figure 39. Model validation by load vs. displacement curves (Type-A, horizontal loading)	37
Figure 40. Model validation by U-bolt strain due to horizontal load (Type-A, horizontal loading)	38
Figure 41. Model validation by strain from rosette strain gage (Type-A, horizontal loading).....	39
Figure 42. Model validation by U-bolt strain due to preload (Type-A, vertical loading)	40
Figure 43. Model validation by load vs. displacement curves (Type-A, vertical loading).....	40

Figure 44. Model validation by U-bolt strain due to vertical load (Type-A, vertical loading)	41
Figure 45. Model validation by strain from rosette strain gage (Type-A, vertical loading).....	42
Figure 46. Model validation by U-bolt strain due to preload (Type-B, horizontal loading)	43
Figure 47. Model validation by load vs. displacement curves (Type-B, horizontal loading).....	43
Figure 48. Model validation by U-bolt strain due to horizontal load (Type-B, horizontal loading)	44
Figure 49. Stress-strain curves of the materials studied during parametric study	46
Figure 50. Parametric study loading directions relative to the vertical direction for the Type-A specimens.....	47
Figure 51. Critical location on pipe (Type-A)	49
Figure 52. Critical location at the angle (Type-B).....	50
Figure 53. Interaction diagram for Type-A specimen	51
Figure 54. Interaction diagram for Type-B specimen.....	52

LIST OF TABLES

Table 1. Material types for laboratory tested specimen.....	11
Table 2. FEM details.....	29
Table 3. Ultimate capacity comparisons	32
Table 4. Ultimate capacity comparisons (calibrated model)	33
Table 5. Materials of interest	45
Table 6. Parametric study results	48

ACKNOWLEDGMENTS

The authors would like to thank the Iowa Department of Transportation (DOT) for sponsoring this project. The assistance of the technical advisory committee, which included Harold Adcock, Mike Todsén, and Mike Nop, was also appreciated throughout the duration of the project.

EXECUTIVE SUMMARY

Objective

The objective of this project was to develop methodologies and/or guidance on how to estimate the capacity of the U-bolt connections specified in the Iowa Department of Transportation's (DOT's) steel overhead sign truss (SOST) design standards.

Problem Statement

The true load capacities of the U-bolt connections used to support the overhead signs are not known, because the bolts are used in ways that do not match the available manufacturer data or the way that manufacturers intended the bolts be used.

Although the Iowa DOT Office of Bridges and Structures is unaware of any U-bolt connection failures since the SOST standards were released in 2011, the load capacities of the U-bolt connections are not known.

Background

The current Iowa DOT SOST design standards utilize U-bolt connections to anchor a four-chord horizontal space truss to support columns at each end of the space truss. The SOST standards also utilize U-bolt connections to attach vertical sign-support members to the front-top and front-bottom chords of the space truss.

The SOST U-bolt dimensional and material properties are substantially the same as those used in the earlier STeel OverHead (STOH) sign truss design standards, which were utilized from about 1970–2011. It is reassuring that the current type of U-bolt connections appear to have performed satisfactorily for more than 40 years. However, there is a growing safety concern due to an ever-increasing need for the Iowa DOT's overhead sign trusses to support larger signs by trusses with even greater span lengths.

Research Description

A comprehensive literature search on the utilization of and modeling of U-bolt connections was conducted for this project, which helped in confirming the research approach.

Using the current Iowa DOT SOST design standards and actual loading conditions, three laboratory tests were conducted on the following two types of critical U-bolt connections that were identified and selected:

- Type-A U-bolt connection used to anchor the bottom chords of the horizontal space truss to supporting columns at each end of the space truss

- Type-B U-bolt connection used to attach vertical sign support members to the front-top and front-bottom chords of the space truss

To simulate the critical load conditions applied on the two types of connections, two Type-A U-bolt connection specimens and one Type-B U-bolt connection specimen were designed with the material and geometric properties used in the SOST design standards. The specimens were fabricated, instrumented, and tested in the Iowa State University Structural Engineering Research Laboratory.

A numerical modeling program was developed to assist in understanding the actual behaviors and failure modes of the U-bolt connections. To further interpret the test results and provide a valid analytical tool for the parametric study to be conducted, finite element models (FEMs) were developed for the specimens.

The results from the FEMs were compared against the load test results to validate the modeling approach. The calibrated models were then used in the parametric study that was performed to understand the behavior of the U-bolt connections with different material properties and subject to various loading conditions.

Given that the laboratory tests on the specimens were conducted and the model calibration was performed based on the most frequently used 3/4-in. diameter U-bolt, the parametric study was also performed for the 3/4-in. diameter U-bolt connection. The parametric study was used to calculate the yield and ultimate capacities of both specimen types (with various material properties and load directions).

Finally, based on the experimental and numerical results, interaction diagrams were developed for designers and engineers to use in capacity estimation of their U-bolt connections under different loading conditions.

Key Findings

Literature Review Leading to Research Approach

- A comprehensive search of available literature indicated few research investigations on the capacity of U-bolt connection in civil engineering. However, related research was found in the fields of mechanical and vehicle engineering.
- Through the literature review, the researchers found that developing an FEM associated and calibrated with laboratory tests is the most commonly used approach to study the behavior of bolt-joined connections/U-bolt assemblies.

- The determination of the element type is a matter of computation time and computer capacity as related to model size. If enough computer time is available, the model with the solid element and surface contact element was found to provide the most accurate results.
- It was also found that model accuracy is sensitive to the definition of the contact behavior. It is essential to correctly model the contact interaction.
- Many approaches could be used to assign the preload (created by torque) to the FEM, including applying thermal strain on the shank or washers, or assigning an initial displacement onto the bottom of the bolt.

Research Results

- The results from both laboratory tests and analytical solutions indicate that different failure modes occur when the loading is in different directions.
- The results from the analytical study show a relatively low yield capacity, but indicate that the details have good ductility before reaching failure.
- The parametric study results indicate that the thread region is the most vulnerable location and that most of the failures start from that region.

Implementation Readiness and Benefits

This research helped to understand the structural behavior and stress distribution of the U-bolt connections used on the Iowa DOT's overhead sign structures subject to various loading conditions. The research results will benefit the Iowa DOT and other state DOTs that utilize similar U-bolt connections in overhead sign support structures.

This research resulted in interaction diagrams that Iowa DOT bridge designers and construction engineers, as well as other bridge owners, consultants, and contractors, can use for overhead sign support structures. The interaction diagrams were created for U-bolt connection capacity estimation under different loading conditions. Engineers can find the capacities by inputting the material type and load resultant direction.

Recommendations for Future Research

The research summarized in the final report represents a major step toward developing a better understanding of the behavior and design of U-bolt connections. However, several questions remain that could be answered by conducting additional research, as follows:

- Additional laboratory tests should be performed on high-strength U-bolts with loading directions of 135° and 180°, because the failure locations predicted by the FEM analyses with high-strength U-bolts are different from those captured in the laboratory tests.
- More experimental and analytical work should be conducted with various loading directions (e.g., 30°, 60°, 120°, and 150°) to study structural behavior subject to various loading directions.
- Given that almost all of the material types appear to have low yield capacity, the fatigue performance of the U-bolt connection should be investigated to understand the impact of repeated loads near the yield load. Additional laboratory tests are recommended to study the fatigue performance of the U-bolt connections.
- Given that both experimental and analytical work were conducted on the 3/4-in. diameter U-bolt, further research is recommended on U-bolt connections with other sizes to obtain the relationship between the U-bolt size and connection capacity.

CHAPTER 1. INTRODUCTION

1.1 Problem Statement

The true load capacities of the U-bolt connections used in the Iowa Department of Transportation's (DOT's) steel overhead sign trusses are not known because the bolts are used in ways that do not match the available manufacturer data or the way that manufacturers intended the bolts be used. Although these U-bolt connections appear to have performed satisfactorily in the past, there has been a growing safety concern in recent years because of the need for overhead sign trusses to support larger signs by trusses with greater span lengths.

As indicated by the Iowa DOT Office of Bridges and Structures, it is imperative to determine if the U-bolt connections have adequate strength to safely perform in current overhead sign support structures, as well as in future ones that will need to resist even greater loads. For example, it is likely that an upcoming highway signing project for the I-35/I-80/IA 141 interchange reconstruction in Urbandale will require two custom overhead sign trusses that must support loads at the limits of the current Iowa DOT standard design. To ensure that these special trusses can safely support the required loads, it will be necessary to know if the U-bolt connections have sufficient strength.

1.2 Background

The current Iowa DOT steel overhead sign truss (SOST) design standards utilize U-bolt connections to anchor a four-chord horizontal space truss to support columns at each end of the space truss. The SOST standards also utilize U-bolt connections to attach vertical sign-support members to the front-top and front-bottom chords of the space truss. Although the Office of Bridges and Structures is unaware of any U-bolt connection failures since the SOST standards were released in 2011, the load capacities of the U-bolt connections are not known.

The SOST U-bolt dimensional and material properties are substantially the same as those used in the earlier Steel OverHead (STOH) sign truss design standards, which were utilized from about 1970–2011. It is reassuring that the current type of U-bolt connections appear to have performed satisfactorily for more than 40 years. However, there is a concern due to an ever-increasing need for the Iowa DOT's overhead sign trusses to support larger signs by trusses with even greater span lengths. It is possible that the actual design loads may already exceed (or may soon exceed) the capacities for the current type of U-bolt connections.

In 2015, the Office of Bridges and Structures and the Bridge Engineering Center at Iowa State University conducted a literature search to determine if any acceptable U-bolt capacity information was available in the form of load test data, computer modeling (i.e., finite element model) results, or verified engineering formulas. When no useful information was found, The Office of Bridges and Structures distributed a questionnaire pertaining to U-bolt capacities to state DOTs through the American Association of State Highway and Transportation Officials (AASHTO) Subcommittee on Bridges and Structures. Fourteen state DOTs responded to the

questionnaire, confirming that little U-bolt load capacity research or theoretical design has been done.

1.3 Objective

The objective of this project was to develop methodologies and/or guidance on how to estimate the capacity of the U-bolt connections specified in the SOST design standards. To achieve the goal, an experimental program was conducted to load test U-bolt connections of the same dimensional and material properties used in the actual SOST design standards.

A numerical modeling program was developed to assist in understanding the actual behaviors and failure modes of the U-bolt connections; these numerical models were validated against the load test data. Based on the experimental and numerical results, interaction diagrams were developed for the purpose of estimating the capacities of the U-bolt connections.

1.4 Research Plan

Five tasks were conducted to meet the objective of the project:

- Task 1 – Technical advisory committee (TAC) establishment
- Task 2 – Experimental program
- Task 3 – Development and validation of finite element models (FEMs)
- Task 4 – Parametric studies and interaction diagram development
- Task 5 – Final report and tech transfer (t2) summary development

These tasks were performed in close communication with the TAC.

1.5 Products

The following products were prepared:

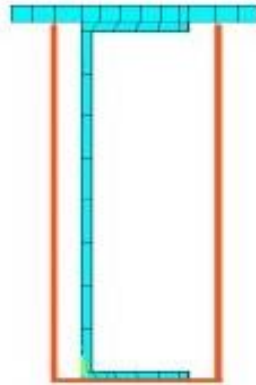
- Quarterly progress reports to the TAC
- Outline of final report (copy to the TAC and to the Iowa DOT Research Engineer)
- Draft final report
- Final report
- T2

CHAPTER 2. LITERATURE REVIEW

2.1 U-bolt Connection

A comprehensive search of available literature indicated few research investigations on the capacity of U-bolt connection in civil engineering. However, related research was found in the fields of mechanical and vehicle engineering.

Diamantoudis and Apostolopoulos (2002) developed an FEM on a U-bolt system that was designed to secure a plate to a truck frame member (see Figure 1).

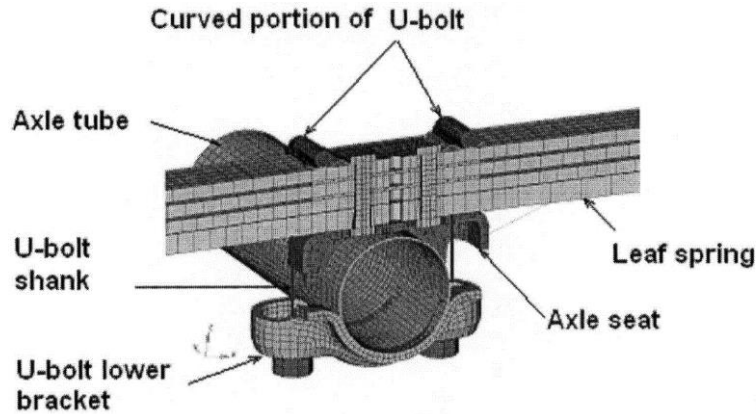


Diamantoudis and Apostolopoulos 2002

Figure 1. Finite element modeling of U-bolt assembly

The objective of this research was to investigate the stress distribution on the U-bolt and C channel, and to determine whether the maximum stress exceeded a certain stress limitation. The results indicated that the maximum stress on the U-bolt occurs on the shank of the U-bolt, and the C channel experienced the highest bending stress at the bottom corner.

Kirby and Charniga (2005) created an FEM of a U-bolt system that used to clamp a leaf spring pack, axle seat, and lower bracket to the axle tube (see Figure 2).

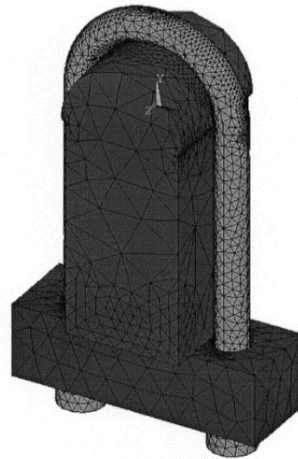


Kirby and Charniga 2005, Copyright © 2005 SAE International, from Shetty 2006

Figure 2. FEM of U-bolted leaf spring assembly

The goal of the research was to address noise concerns by investigating the stresses in the leaf spring when it was subject to twisting. The analytical results were output and compared to the experimentally measured results on the axle seat.

Shetty (2006) investigated the load capacity and stress distribution on a suspension component in the onboard weighing system of off-highway log trucks. The suspension component of interest consisted of a trunnion saddle, a U-bolt, and a leaf spring (see Figure 3).



Shetty 2006

Figure 3. FEM of U-bolt connection

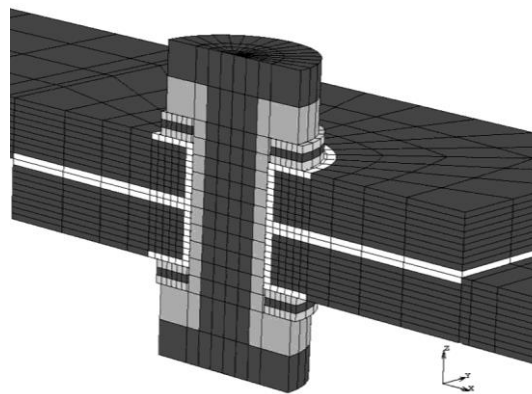
During the research, laboratory tests were conducted to collect strain data from the suspension components of the off-highway log tractor. The suspension system specimen was installed into a log truck and loaded with the weight of a slip-on water tank. An FEM was developed using ANSYS software to determine the locations on the U-bolt surface that would provide the largest strain. The results indicated that the top of the curved portion of the U-bolt showed the maximum strain and was recommended as a preferred position for a future monitoring project.

2.2 Finite Element Modeling (FEM)

In the literature, the finite element method is the most common approach utilized (typically in combination with laboratory tests) to study the stress distribution on U-bolt assemblies of interest. However, different modeling approaches were adopted by the various researchers with the consideration of differences in their research objectives, efficiency in computation time, and model size capacity of the computer, etc.

For example, in the models developed by Diamantoudis and Apostolopoulos (2002) and Kirby and Charniga (2005), the U-bolt shank and curve were modeled using a two-dimensional (2D) beam element, and the other components were modeled using a three-dimensional (3D) solid element. However, Shetty (2006) created the whole U-bolt assembly using only 3D quadratic tetrahedral solid elements. On the model developed by Shetty (2006) the contact behaviors between the U-bolt and leaf spring block, and between the leaf spring block and trunnion saddle were modeled using surface-to-surface contact elements. The preload due to the fastening torque was simulated by assigning an appropriate coefficient of thermal expansion and specifying a temperature change on the shank of the U-bolt.

Although research conducted on U-bolt connections is sparse, studies on normal steel bolts are quite abundant. The modeling technique commonly used for normal bolts can provide valuable reference to the finite element modeling of the U-bolt connection. For example, McCarthy and McCarthy (2005) and McCarthy et al. (2005) developed a 3D FEM to study the effects of bolt-hole clearance on the mechanical behavior of bolted composite joints. Nonlinear FEMs consisting of the bolt, two plates, a nut, and washers (as shown in Figure 4) were developed on a single-bolt, single-lap connection to evaluate the modeling techniques.

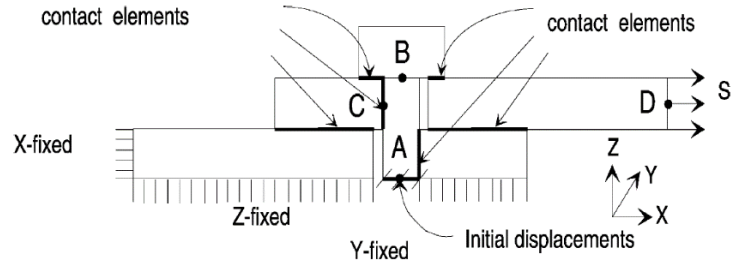


McCarthy et al. 2005, Copyright © 2004 Elsevier Ltd. All rights reserved. Used with permission from Elsevier.

Figure 4. FEM of bolt connection

The analytical results were compared against experimental results to determine the various parameters of the material properties and the contact mechanism. The preload was applied by assigning an orthotropic thermal expansion coefficient to the washer (allowing the thermal expansion/contraction only in the direction parallel to the longitudinal axial of bolt) and applying a positive temperature change onto the washer.

Ju et al. (2005) created a 3D elasto-plastic FEM to study the structural behavior of a butt-type steel bolted joint. Both bearing-type and slip-critical type connections were modeled using 3D solid elements for the bolt and plate. Contact elements were used to model the interface. The boundary conditions and locations of the contact elements are shown in Figure 5.

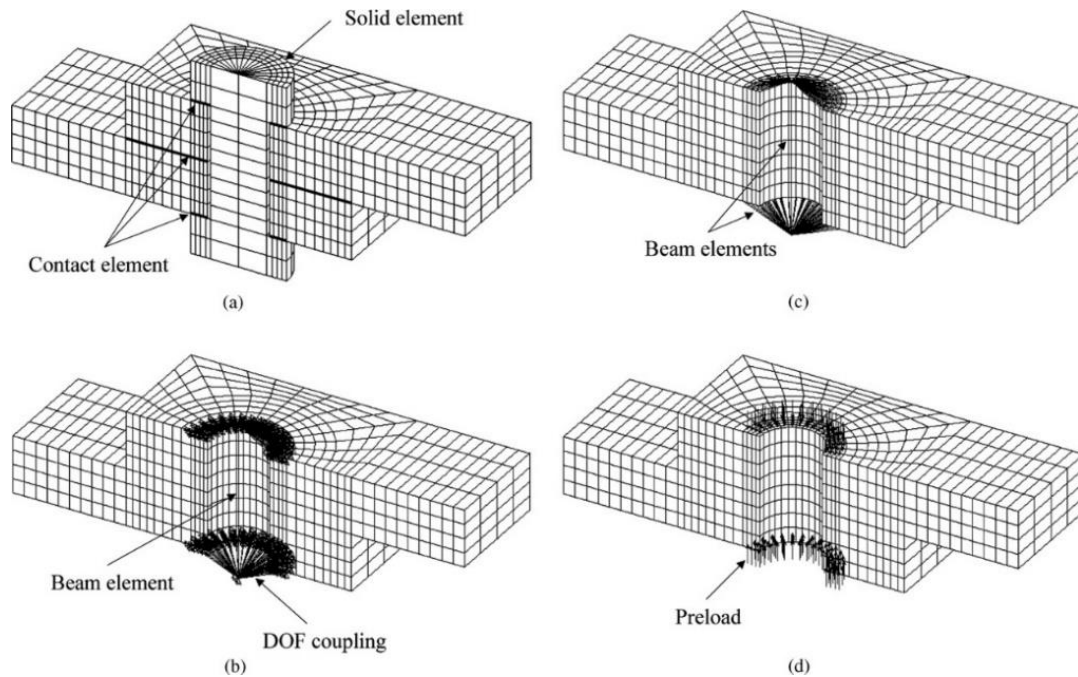


Ju et al. 2005, Copyright © 2003 Elsevier Ltd. All rights reserved. Used with permission from Elsevier.

Figure 5. Boundary conditions and contact surfaces

To account for the shear force being transferred from the plate directly to the bolt, a contact element was assigned at the vertical interface between the bolt and the plate. The preload was modeled by applying an initial displacement at Point A in Figure 5.

Kim et al. (2007) performed finite element analysis on a large marine diesel engine utilizing ANSYS software. To determine the best modeling technique for the bolted joint structure, four types of joint models, including a solid bolt model, a coupled model, a spider bolt model, and a no-bolt model, were developed and evaluated (see Figure 6).



Kim et al. 2007, Copyright © 2006 Elsevier Inc. All rights reserved. Used with permission from Elsevier.

Figure 6. Small-scale FEM of bolt connection

The preload due to the fastening torque was modeled using thermal strain, and a surface-to-surface contact element was used at the interface between the head/nut and the flanges. The results indicated that the solid bolt model, which meshes the U-bolt shank and curve with the 3D solid element, provided the most accurate stress distribution on the U-bolt when compared with the experimental results.

2.3 Summary

Based on the results of the literature review, the researchers found that developing an FEM associated and calibrated with laboratory tests is the most commonly used approach to study the behavior of bolt-joined connections. The determination of the element type is a matter of computation time and computer capacity as related to model size. If enough computer time is available, the model with the solid element and surface contact element was found to provide the most accurate results.

It was also found that model accuracy is sensitive to the definition of the contact behavior. It is essential to correctly model the contact interaction. Many approaches could be used to assign the preload (created by torque) to the FEM, including applying thermal strain on the shank or washers, or assigning an initial displacement onto the bottom of the bolt.

CHAPTER 3. LABORATORY TESTS

The objective of the laboratory testing conducted in this work was to monitor the structural behavior of the U-bolt, capture the failure mode when the bolt is subject to loading in different directions, and provide data for the calibration of the FEM.

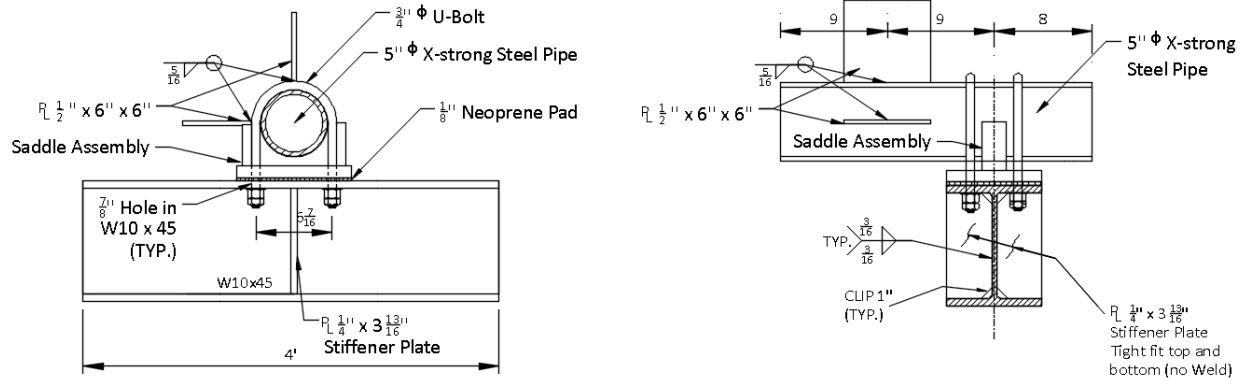
Per the current Iowa DOT SOST design standards and actual loading conditions, two types of critical U-bolt connections were identified and selected for experimental evaluation: the Type-A U-bolt connection used to anchor the bottom chords of the horizontal space truss to supporting columns at each end of the space truss and the Type-B U-bolt connection used to attach vertical sign support members to the front-top and front-bottom chords of the space truss.

To simulate the critical load conditions applied on the two types of connections, two Type-A U-bolt connection specimens and one Type-B U-bolt connection specimen were fabricated, instrumented, and tested in the Iowa State University Structural Engineering Research Laboratory.

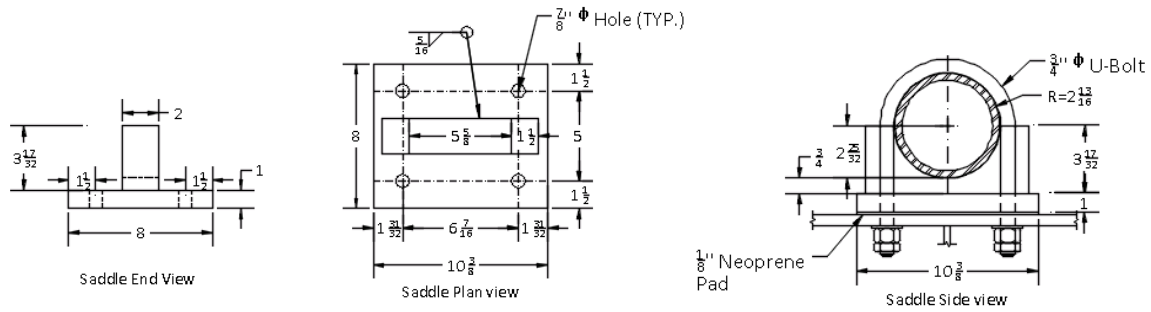
3.1 Type-A Specimens

3.1.1 Specimen Description

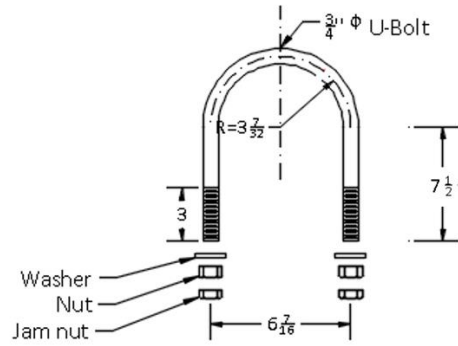
The specimens were designed with the material and geometric properties used in the actual SOST design standards. As shown in Figure 7 and Figure 8, the Type-A specimens consisted of a W-shaped steel beam, a saddle assembly, a steel pipe with two steel plates, and the U-bolt components.



(a) Specimen views and profiles



(b) Saddle views and profiles



(c) U-bolt details

Figure 7. Type-A U-bolt specimen design



Figure 8. Type-A specimens

The material designation and properties for each component are shown in Table 1.

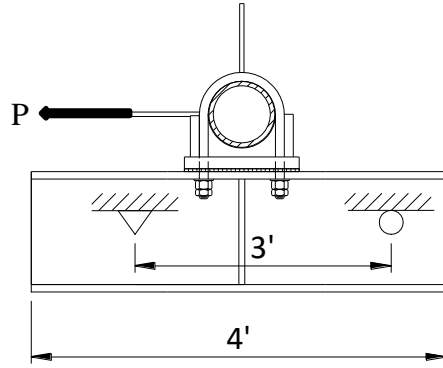
Table 1. Material types for laboratory tested specimen

Part	Steel Grade*	Yield Strength (ksi)	Ultimate Strength (ksi)	Initial Young's Modulus (ksi)
U-bolt	A36	36	65	29,000
Pipe	A53-B	35	60	29,000
Saddle	A572-50	50	65	29,000
Load plate	A36	36	65	29,000
W-shaped beam	A992	50	65	29,000
Angle	A36	36	65	29,000

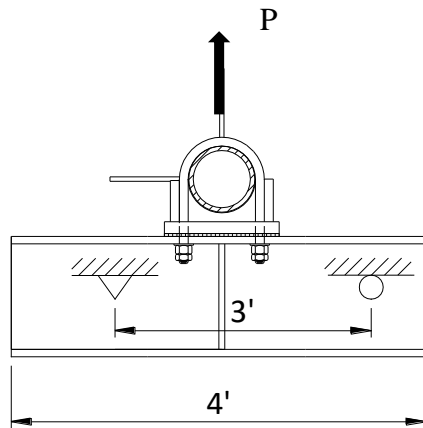
*Although multiple types of steel with different yield and ultimate strength are being used for the U-bolt on actual SOST designs in Iowa, the tests used A36 steel for the experimental study and calibration of the FEM. The performance of other types of steel were evaluated during the analytical parametric study.

3.1.2 Loading Configuration

Two Type-A connection specimens were fabricated and tested. One of the Type-A connection specimens was loaded in the horizontal direction as shown in Figure 9-a, and the other one was loaded in the vertical direction as shown in Figure 9-b.



(a) Force parallel to the W-shaped beam (horizontal loading)



(b) Force perpendicular to the W-shaped beam (vertical loading)

Figure 9. Load configurations on Type-A connection specimens

The loads were applied on the plates welded to the pipe—simulating the loading mechanism in actual field installations (see Figure 10).



(a) Type-A specimen subjected to horizontal load



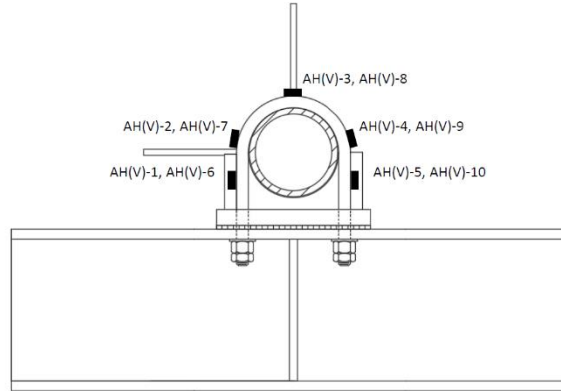
(b) Type-A specimen subjected to vertical load

Figure 10. Type-A specimen setup before testing

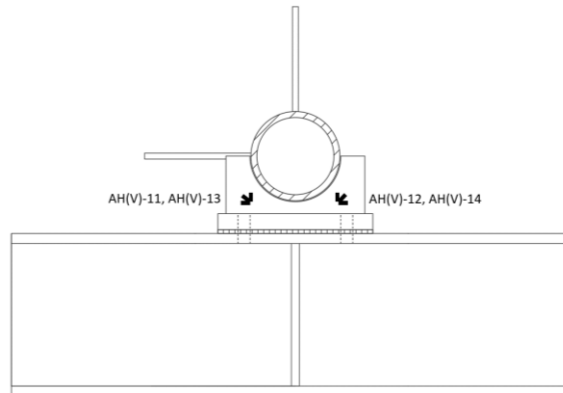
Before the application of the horizontal and vertical loads, a preload was applied by fastening the U-bolt utilizing a 1-ft long (approximate) wrench with the full effort of a human. The full effort of this person was tested using a net loading cell and resulted in about 30 lbf. The total torque applied on each shank was about 30 lbf ft.

3.1.3 Instrumentation

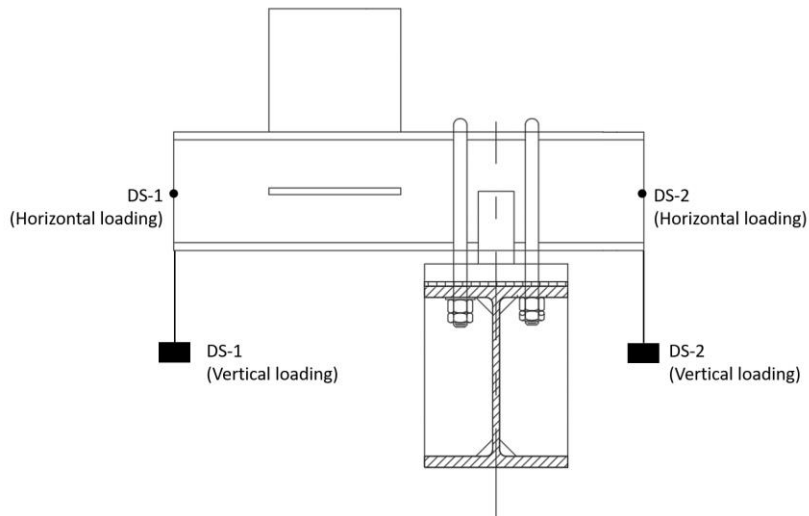
For both tests on the Type-A specimens, the instrumentation plan was the same, as shown in Figure 11.



(a) Straight foil strain gages



(b) Rosette foil strain gages



(c) Displacement transducers

Figure 11. Instrumentation on Type-A specimen

Ten uniaxial foil strain gages and four rosette gages were installed on each specimen. To measure the strain change along the axis of the U-bolt, five uniaxial foil gages were installed on each U-bolt (shown in Figure 11-a) with three at the curved part and two on the shanks at about 1.5 in. above the top surface of the saddle. The four rosette gages were installed at the sides of

the saddle to measure the strain on the surface in multiple directions. In addition, two displacement transducers were used to measure the displacement change as shown in Figure 11-c. The displacement transducers were placed at the two ends of the pipe and were used to measure the displacement change in the loading directions.

The labels were designated so that, A and B denote specimen type, H and V denote the loading direction in horizontal and vertical directions, respectively, and DS denotes the displacement transducers.

On the Type-A specimen, AH-1 to AH-10 and AV-1 to AV-10 are the straight foil strain gage attached on the U-bolt with AH-1 to AH-5 and AV-1 to AV-5 on the U-bolt near the loading side, and AH-6 to AH-10 and AV-6 to AV-10 on the other U-bolt.

The four rosette strain gages were designated from AH-11 to AH-14, and AV-11 to AV-14. AH-11, AH-12, AV-11 and AV-12 were placed near the loading side, and AH-13, AH-14, AV-13 and AV-14 were placed on the other side.

3.1.4 Test Results

Type-A Specimen Subject to Horizontal Loading

During the application of the preload, the strain change on the U-bolt was measured using the uniaxial foil strain gages attached along the axis of the U-bolt. Figure 12 shows the strain induced by the preload.

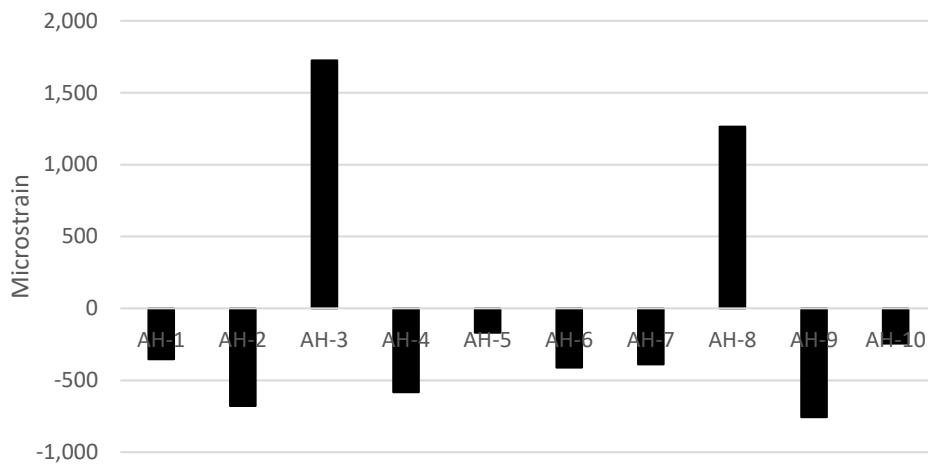


Figure 12. U-bolt strain due to preload (Type-A, horizontal loading)

The strain gages AH-3 and AH-8 attached on the top of the U-bolt captured the maximum strain in tension at about 1,250 to 1,750 microstrain. The other gages showed strain in compression due to the bending effect.

The specimen was then loaded subject to the horizontal load until failure with an ultimate capacity of 36 kips. The specimen broke in a shear-type failure of the U-bolt shanks (on the loading side) induced by the relative displacement between the saddle and the top flange of the W-shaped beam (see Figure 13).



Figure 13. Shear failure on the U-bolt shanks (Type-A, horizontal loading)

Figure 14 shows the force vs. displacement curves from the testing.

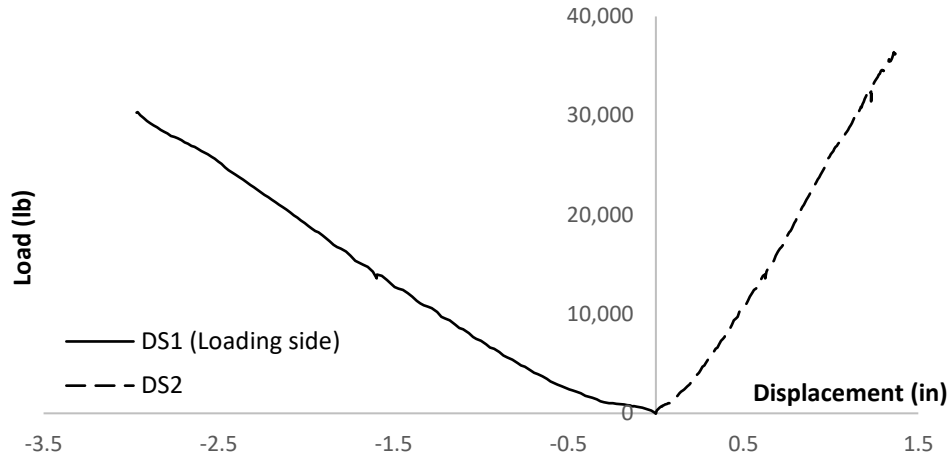


Figure 14. Load vs. displacement curves (Type-A, horizontal loading)

Due to the short extension length of the stringer in DS-1, the data beyond 30 kips was not able to be captured from DS-1. DS-2 kept functioning until the end of the test. Figure 15 shows the strain change along the axis of the U-bolt vs. the applied load.

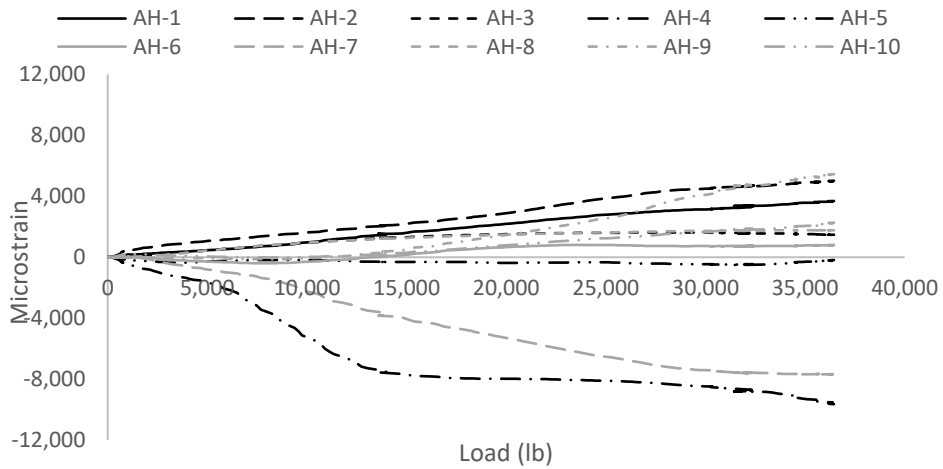


Figure 15. U-bolt strain due to horizontal load (Type-A, horizontal loading)

Figure 16 shows the strain data measured from the rosette gages attached on the sides of the saddle.

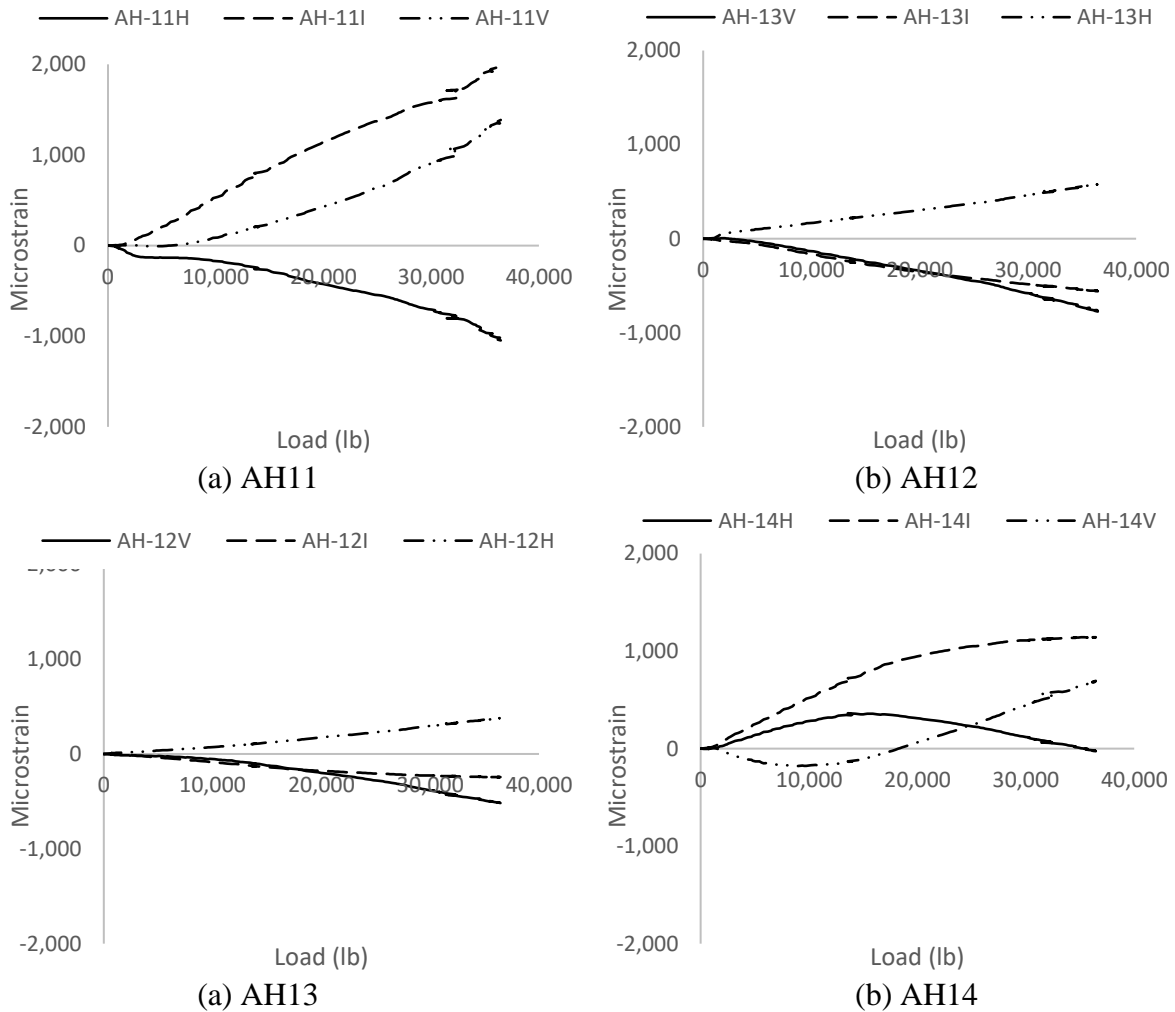


Figure 16. Strain from rosette strain gage (Type-A, horizontal loading)

It is obvious that, compared to the strains on the U-bolt, the surface stains on the saddle are very small even at the ultimate loading stage.

Type-A Specimen Subject to Vertical Loading

The second Type-A specimen was preloaded following the same approach used on the first Type-A specimen and then loaded in the vertical direction. Figure 17 shows the strain change on the U-bolt induced by the preload.

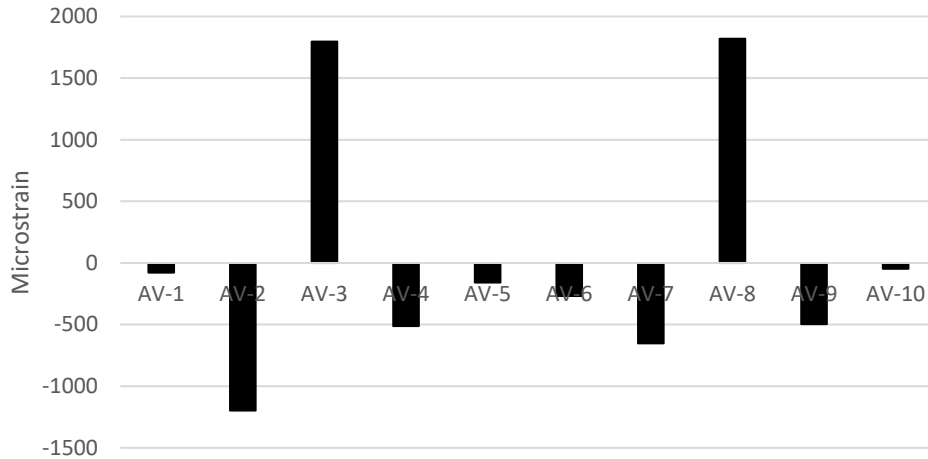


Figure 17. U-bolt strain due to preload (Type-A, vertical loading)

The data shows similar behaviors as those shown in the previous Figure 12 and that the strains on the top of the curved part are in tension with a maximum magnitude of about 1,750 microstrain, while the others are in compression.

During the vertical load test, both U-bolts were tested separately since the test on one U-bolt did not induce any significant loading on the other one. Figure 18 shows the failure modes for the two vertical loading tests.

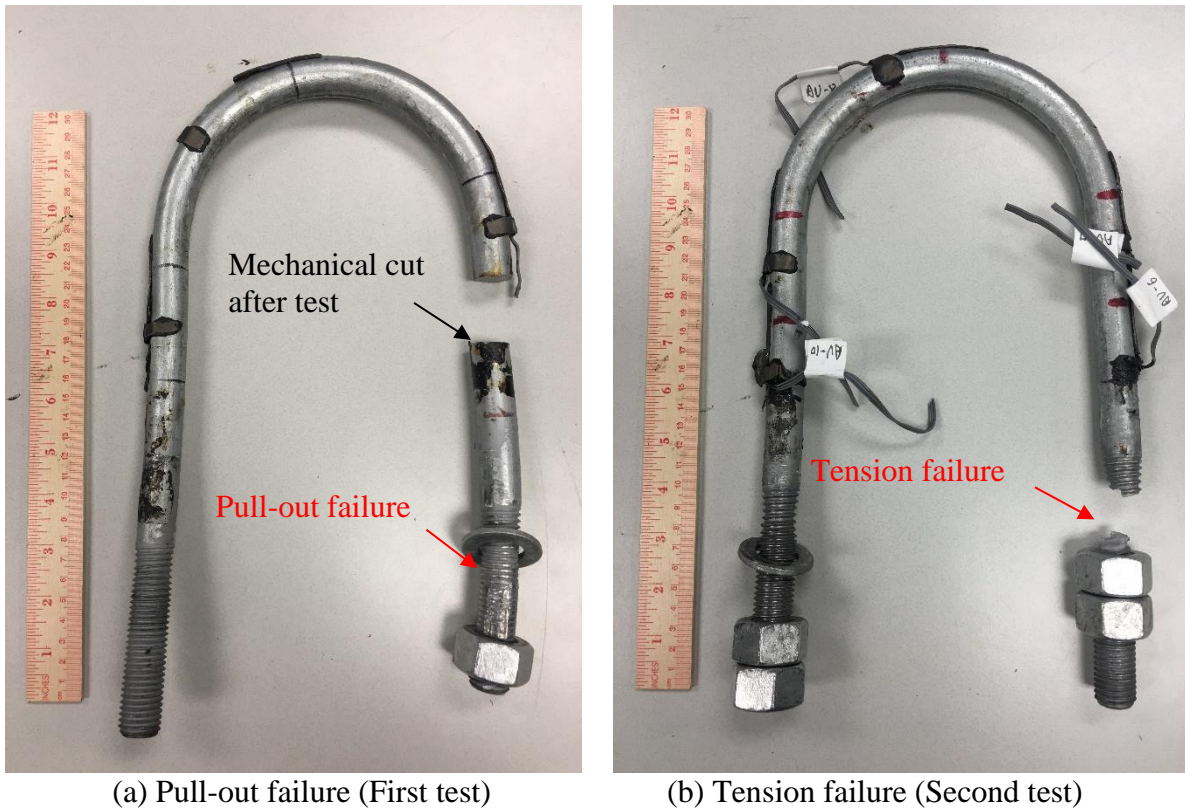


Figure 18. Failure Model (Type-A, vertical loading)

In the first test, only one nut was used to fasten each U-bolt leg, and this test resulted in a pull-out failure when the load reached 25 kips. Because of this, the second test was set up utilizing two 3/4 in. nuts on each shank. The U-bolt broke with a tension failure at a thin cross-section (with a design diameter of 0.63 in. and a cross-sectional area of 0.31 in²) in the thread region when the loading was 24 kips. The results indicated that the ultimate load in the first test is very close to the tensile capacity of the U-bolt, although the pull-out failure occurred right before that.

Figure 19 shows the load versus displacement data.

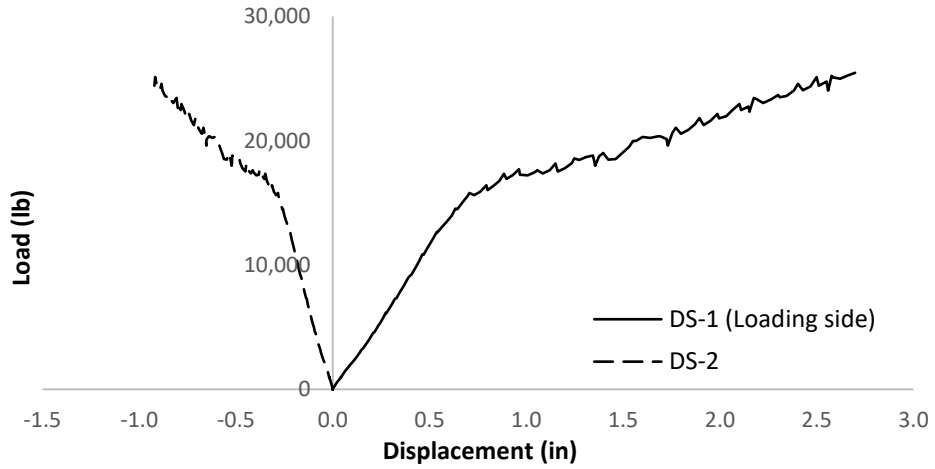


Figure 19. Load vs. displacement curves (Type-A, vertical loading)

Figure 20 and Figure 21 show the strain data measured from U-bolt and saddle, respectively.

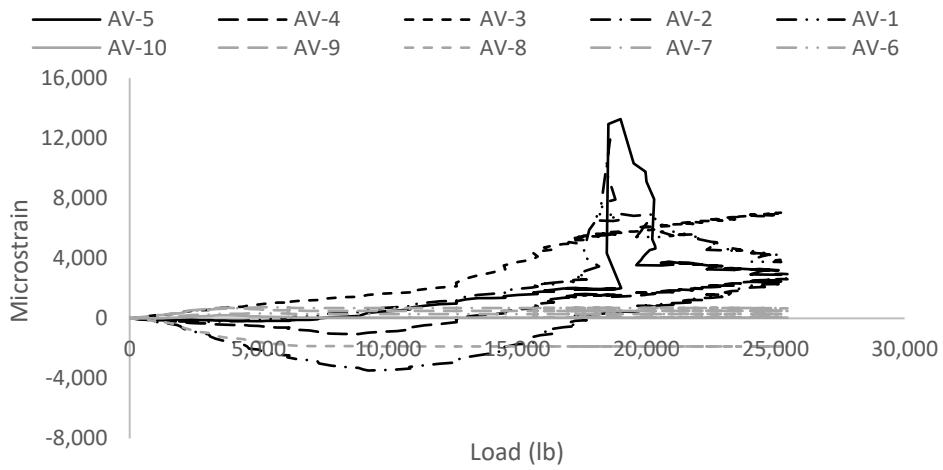


Figure 20. U-bolt strain due to vertical load (Type-A, vertical loading)

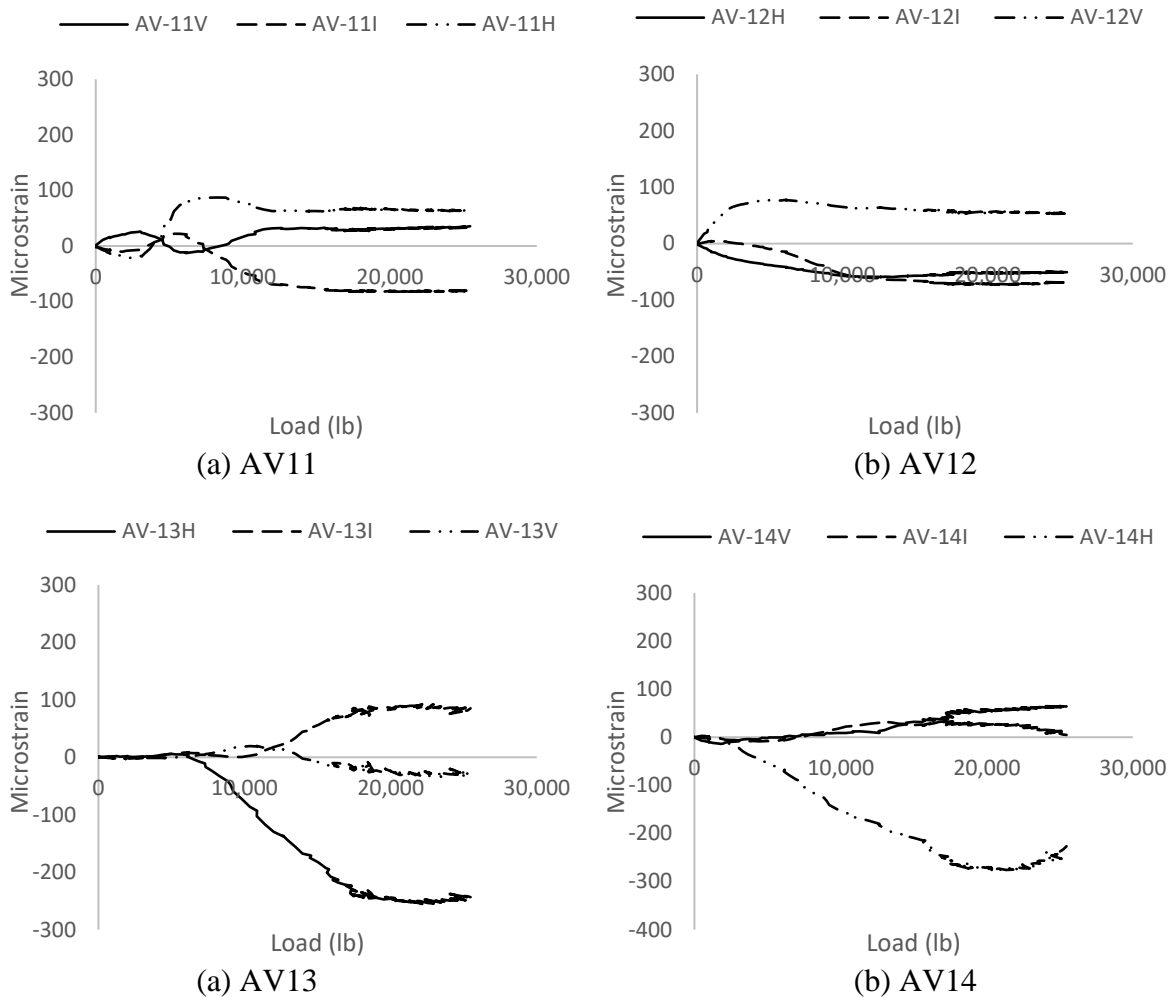


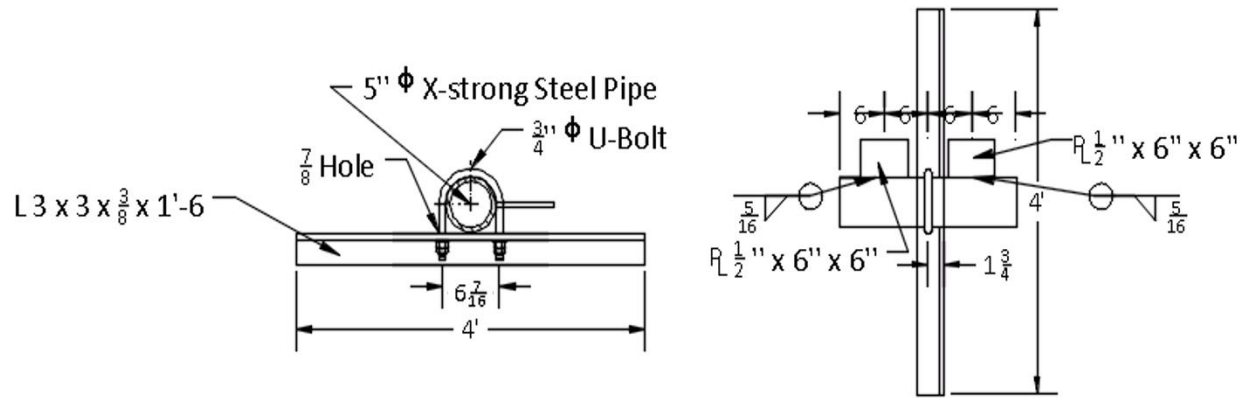
Figure 21. Strain from rosette strain gage (Type-A, vertical loading)

It can be seen from Figure 20 that AV-1 and AV-5, which were placed at the shank of the U-bolt and very close to the failure location, experienced a significantly large strain when loading reached about 18 kips and then lost function because of the functional measurement range of the gage (10,000 microstrain). All of the data shown in Figure 17, Figure 19, Figure 20, and Figure 21 were captured from the first vertical load test. In the second vertical load test, only the ultimate capacity was measured.

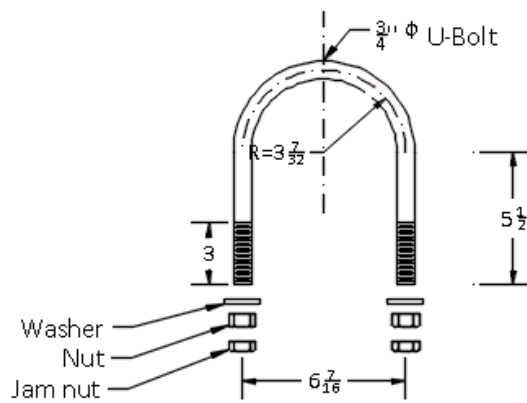
3.2 Type-B Specimen

3.2.1 Specimen Description

As shown in Figure 22 and Figure 23, the Type-B specimen consisted of an angle, a steel pipe, two steel plates, and the U-bolt components.



(a) Specimen views and profiles



(b) U-bolt details

Figure 22. Type-B U-bolt specimen



Figure 23. Type-B specimen

The material type for each component was shown previously in Table 1. The angle was fabricated using A36 steel and the other components were manufactured utilizing the same materials as those used for the Type-A specimen.

3.2.2 Loading Configuration

The Type-B specimen was first loaded with the preload in the same way as the Type-A specimens, and then loaded with the horizontal load as shown in Figure 24 and Figure 25.

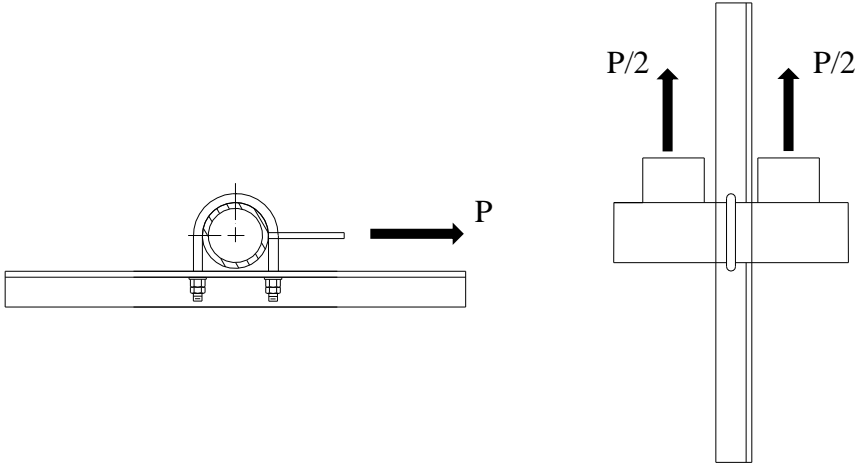


Figure 24. Type-B specimen: force parallel to the angel (horizontal loading)

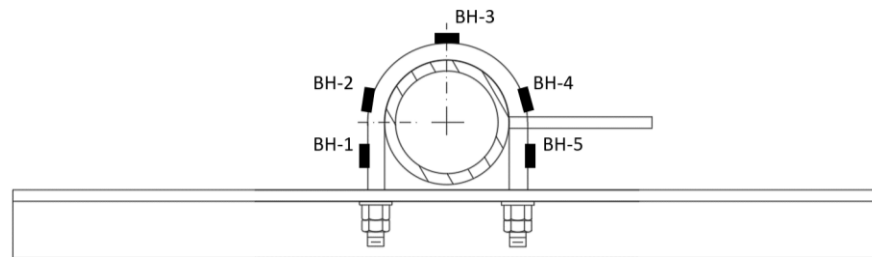


Figure 25. Type-B specimen setup before testing

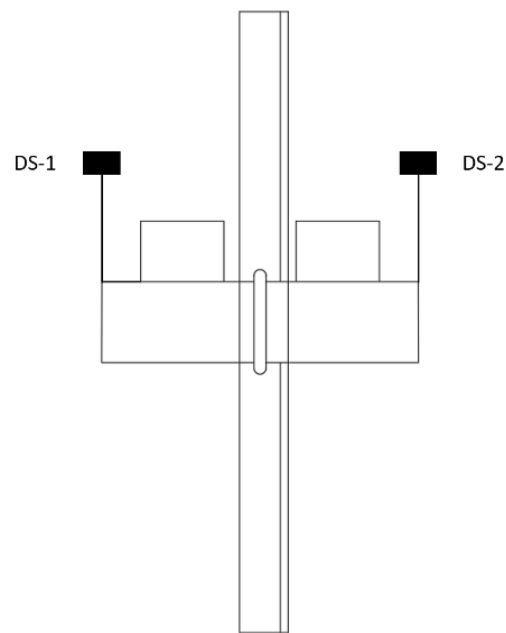
The horizontal load was evenly applied on the two plates simultaneously.

3.2.3 Instrumentation

Figure 26 shows the instrumentation plan on the Type-B specimen.



(a) Straight foil strain gages



(b) Displacement transducers

Figure 26. Instrumentation on Type-B specimen

Five uniaxial foil strain gages were attached along the axis of the U-bolt on the exterior side as shown in Figure 26-a. Two displacement transducers were used to measure the displacement in the horizontal direction as shown in Figure 26-b.

3.2.4 Test Results

Figure 27 shows the strain measured on the U-bolt induced by the preload.

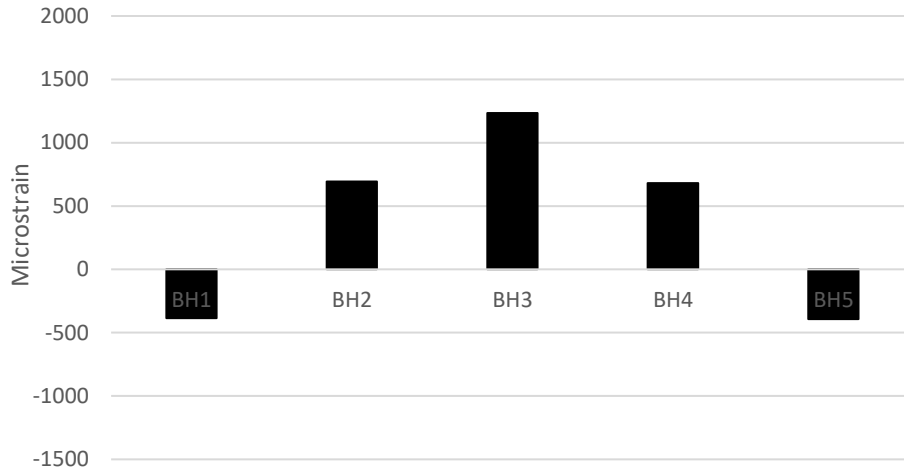


Figure 27. U-bolt strain due to preload (Type-B, horizontal loading)

Similar to the Type-A specimens, the maximum strain occurred at the top of the curved part of the U-bolt with a magnitude of about 1,250 microstrain. Subject to the horizontal load, the U-bolt on the Type-B specimen failed in the threaded region on the front leg (near the loading plate) with a shear failure as shown in Figure 28.



Figure 28. Shear failure on the U-bolt shanks (Type-B, horizontal loading)

The total ultimate load carried by the specimen was about 35 kips.

Figure 29 shows load versus displacement curves for the Type-B specimen subject to the load.

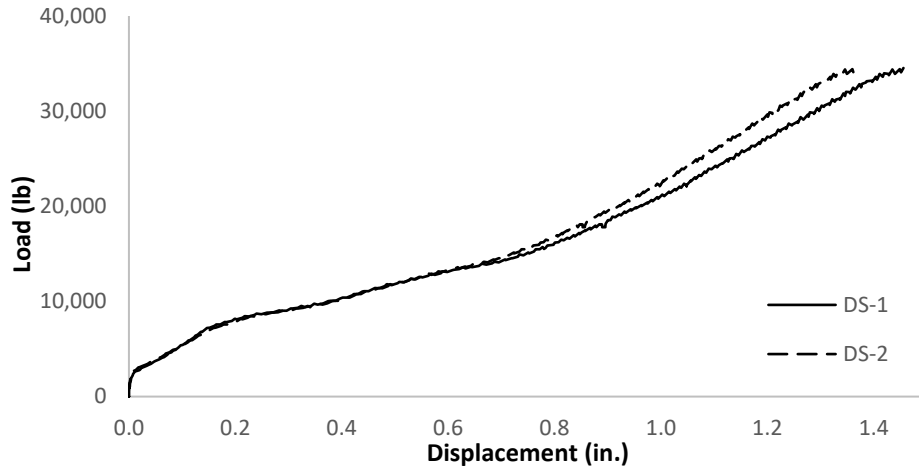


Figure 29. Load vs. displacement curves (Type-B, horizontal loading)

It can be seen that, before the load reached 18 kips, the specimen was loaded symmetrically, but, after that, a small difference in the displacement between the two ends of the pipe appeared.

Figure 30 shows the strain change on the U-bolt versus the loading.

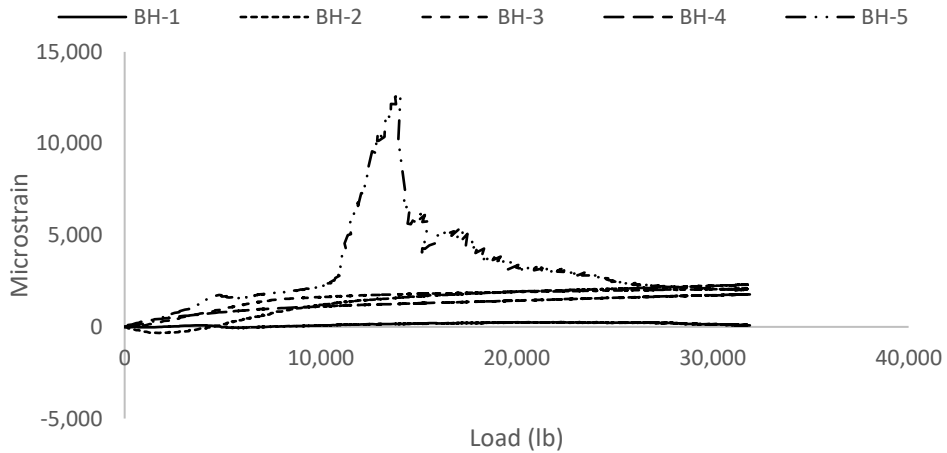


Figure 30. U-bolt strain due to horizontal load (Type-B, horizontal loading)

The strain gage BH-5 was installed on the front shank near the ultimate failure point. It can be seen that, when the load was about 10 kips, a significant plastic deformation occurred in that area. After that, the gage lost function because of range limitations (10,000 microstrain).

CHAPTER 4. MODEL DEVELOPMENT AND VALIDATION

To further interpret the test results and provide a valid analytical tool for the parametric study conducted in the next step, FEMs were developed for the specimens. The results from the FEMs were compared against the test results to validate the modeling approach.

4.1 Model Development

4.1.1 Type-A Specimen

A 3D nonlinear FEM was developed using the commercially available software ANSYS. All steel parts were modeled using Solid185 elements. Table 2 lists the material properties for each component.

Table 2. FEM details

	Steel Grade	Element Type	Yield Strength (ksi)	Ultimate Strength (ksi)	Initial Young's Modulus (ksi)	Specimen Type
U-bolt	A36	Solid185	36	65	29,000	Type-A & -B
Pipe	A53-B	Solid185	35	60	29,000	Type-A & -B
Saddle	A572-50	Solid185	50	65	29,000	Type-A
Load plate	A36	Solid185	36	65	29,000	Type-A & -B
W-shaped beam	A992	Solid185	50	65	29,000	Type-A
Angle	A36	Solid185	36	65	29,000	Type-B
U-bolt (calibrated)	A36	Solid185	60	100	29,000	Type-A & -B
Pipe/U-bolt interface		Surface Contact Element				Type-A & -B
Saddle/pipe interface		Surface Contact Element				Type-A
Pipe/angle interface		Surface Contact Element				Type-B
Saddle/beam interface		Surface Contact Element				Type-A
Nuts and beam interface		Surface Contact Element				Type-A & -B
Shank and side of saddle and top flange of beam		Surface Contact Element				Type-A & -B

Since the FEM is a highly nonlinear model with large deformation, the true stress-strain curve, which was converted based on the engineering stress-strain relation, was input into the model. The engineering stress and strain that were in the engineering software application neglect the necking effect, were established with an initial Young's modulus of 29,000 ksi and a peak strength strain of 0.2 for each component. The true stress and strain, which consider the necking effect, were calculated using equation (1) and equation (2).

$$\epsilon_{true} = \ln(1 + \epsilon_{engineering}) \quad (1)$$

$$\sigma_{true} = \sigma_{engineering} \times (1 + \epsilon_{engineering}) \quad (2)$$

where, ϵ_{true} is the true strain; $\epsilon_{engineering}$ is the engineering strain; σ_{true} is the true stress and $\sigma_{engineering}$ is the engineering stress. Figure 31 shows both engineering and true stress-strain curves for each component.

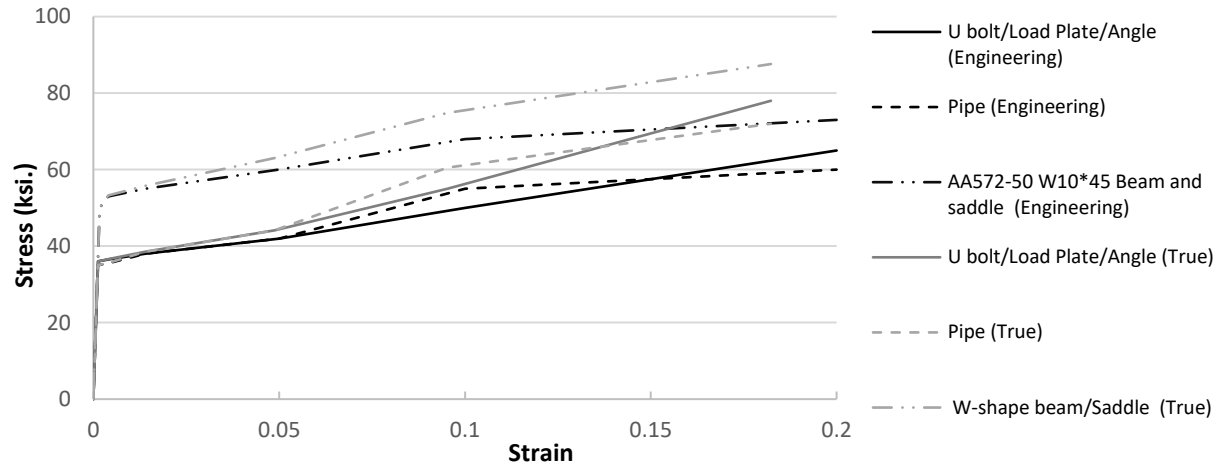


Figure 31. Engineering and true stress-strain data

Surface contact element pairs Conta173/Target170 were used to model the interaction between the U-bolt and pipe, saddle and pipe, saddle and beam, nuts and beam, shank and sides of the saddle, and top flange of the W-shaped beam. The contact properties were defined with a steel-to-steel friction coefficient of 0.75 and 0 cohesion. Since the W-shaped beam was tied-down on the ground with high pressure during the test (see previous Figure 10) and resulted in high friction resistance between the bottom flange of the W-shaped beam and the ground, the bottom flange of the W-shaped beam was fixed on the FEM. The preload was applied onto the nut/washer elements in the same way as that used by McCarthy and McCarthy (2005) and McCarthy et al. (2005), and the horizontal/vertical loads were applied on the plate (welded on the pipe) gradually, until failure. Figure 33 shows the FEM of the Type-A specimen.

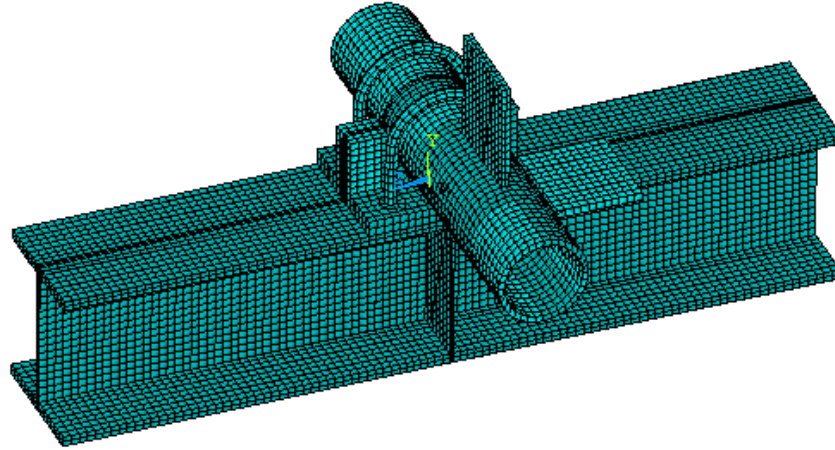


Figure 32. FEM of Type-A specimen

4.1.2 Type-B Specimen

The Type-B model was developed in the same manner as the Type-A model. The stress strain curve for the angle was shown previously in Figure 31. Figure 33 shows the FEM of the Type-B specimen.

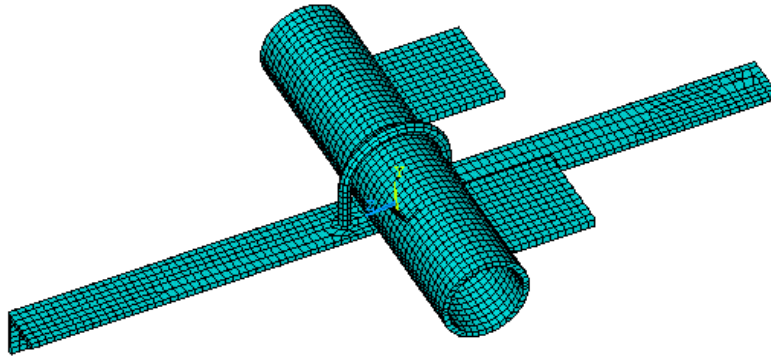


Figure 33. FEM of Type-B specimen

4.2 Model Validation

4.2.1 U-Bolt Steel $f_y = 36$ ksi, $f_u = 60$ ksi

The model was first analyzed with the standard material properties of $f_y = 36$ ksi and $f_u = 60$ ksi for A36 steel. However, the analytical results showed a difference when compared to the experimental results. Figure 34 compares the force vs. displacement curves on the Type-A specimen subject to the vertical load.

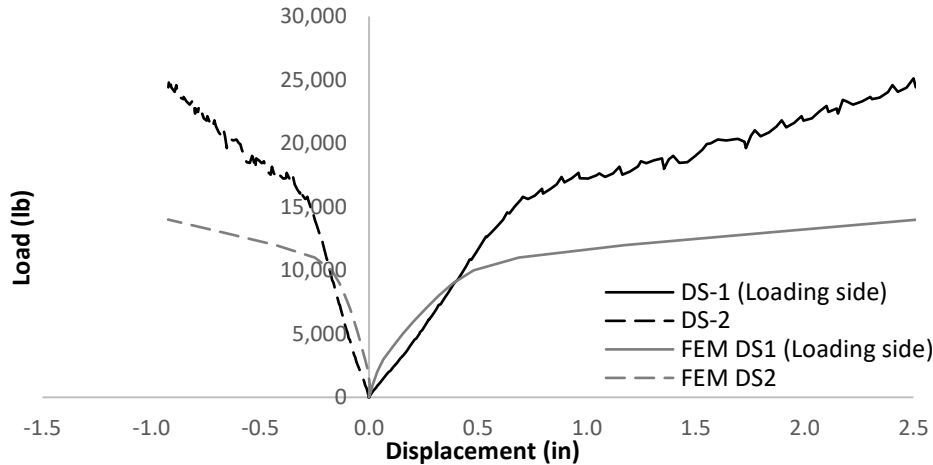


Figure 34. Model validation with load vs. displacement curves (Type-A, vertical loading)

It is apparent that the experimental results indicated a system yield point at about 18 kips, but the FEM results showed a system yield point when load was about 10 kips.

Table 3 compares the ultimate capacities between the analytical and experimental results.

Table 3. Ultimate capacity comparisons

Specimen	Loading	Ultimate Capacity		Difference
		(Test)	(FEM)	
Type-A	Horizontal	38 kips	20 kips	47%
Type-A	Vertical	24 kips	15 kips	38%
Type-B	Horizontal	35 kips	20 kips	42%

For the Type-A specimen subjected to the vertical loading and the Type-B specimen under horizontal loading, the failure on the tested specimens occurred in the thread region at the thin cross-section (with an area of about 0.31 in^2), while the FEM did not include the thread and had a consistent cross-section area of about 0.44 in^2 . To account for the thin cross-section at the thread region, failure was identified when stress at the thread achieved a ratio of $0.31 \div 0.44 \times f_u$. The corresponding strain was used to find the failure loading. For the two Type-A specimens and the Type-B specimen, the FEM resulted in an ultimate capacity of 38% to 47% lower than the test results.

4.2.2 U-Bolt Steel $f_y = 70 \text{ ksi}$, $f_u = 110 \text{ ksi}$

Because of the significant difference between the experimental and analytical results as discussed in Section 4.2.1, the stress-strain curve for the U-bolt was calibrated to $f_y = 70 \text{ ksi}$ and $f_u = 110 \text{ ksi}$ with the stress-strain curve as shown in Figure 35.

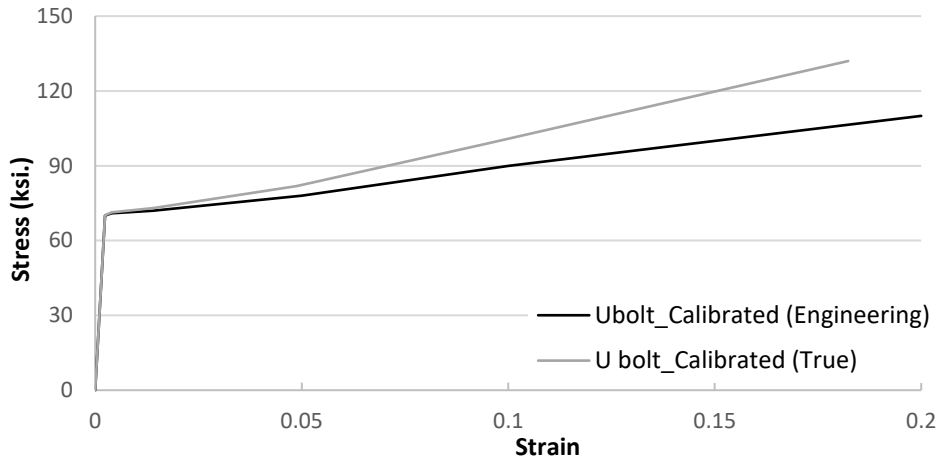


Figure 35. Stress-strain data for the U-bolt on the calibrated model

Table 4 compares the ultimate capacities from the calibrated model against the experimental results for each test.

Table 4. Ultimate capacity comparisons (calibrated model)

Specimen	Loading	Ultimate Capacity (Test)	Ultimate Capacity (FEM)	Difference
Type-A	Horizontal	38 kips	36 kips	5%
Type-A	Vertical	24 kips	26 kips	8%
Type-B	Horizontal	35 kips	34 kips	2%

The two Type-A specimens and the Type-B specimen show a small difference of 2% to 8%.

Figure 36 shows the von Mises strain distribution on the U-bolt after preload.

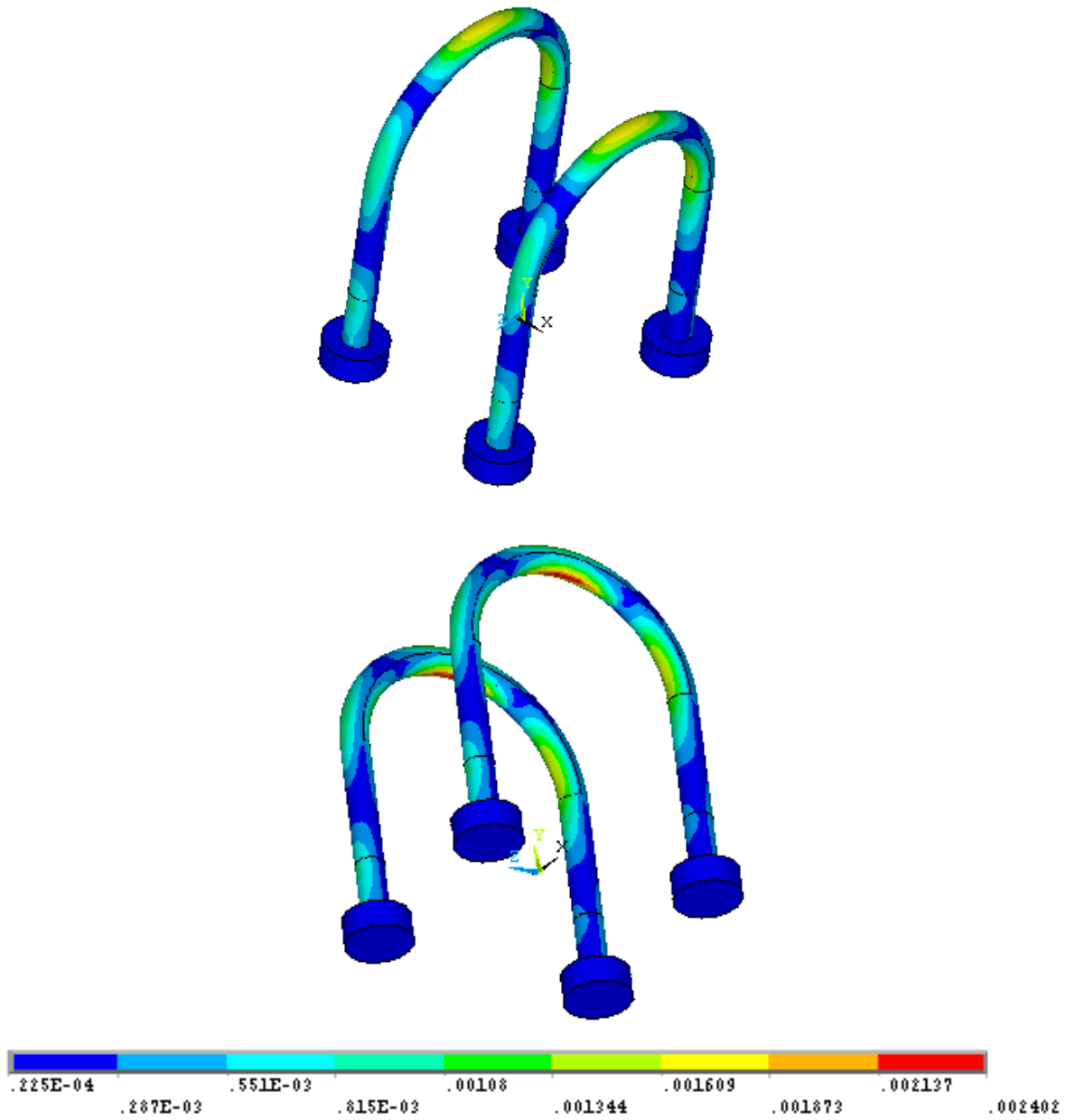
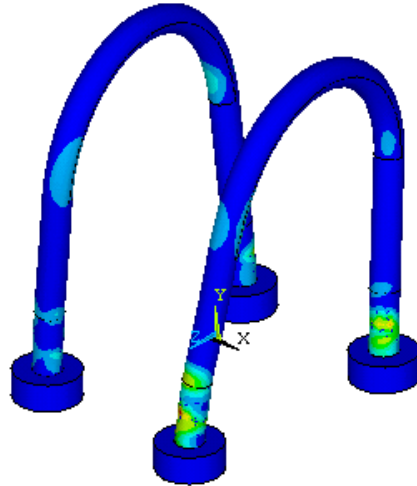
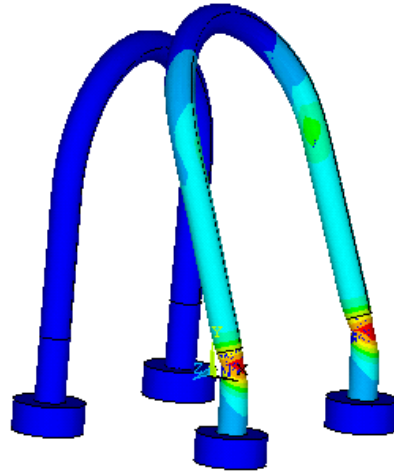


Figure 36. von Mises strain on the U-bolt after preload

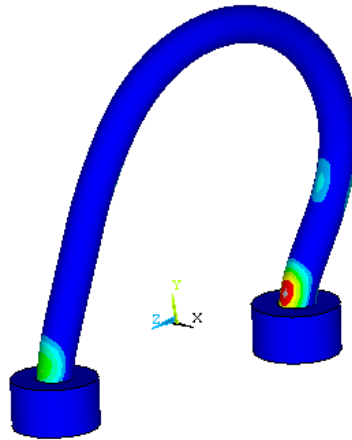
The maximum strain after preload occurs at the interface between the U-bolt and pipe with a stress concentration resulting in a strain of about 0.0024. Figure 37 shows the von Mises strain distribution on the U-bolt at the ultimate stage with an exaggerated deformed shape.



(a) Type-A specimen subject to horizontal loading



(b) Type-A specimen subject to vertical loading



(c) Type-B specimen subject to horizontal loading

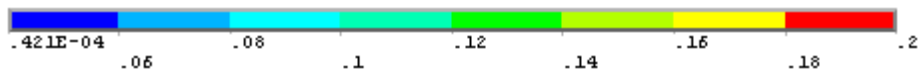


Figure 37. von Mises strain on the U-bolt at ultimate stage

Although Figure 37-b, shows the maximum strain occurs at the shank (above the thread region), a detailed observation indicates that the thread region (blocked by the nuts) achieved a stress equal to $0.31 \div 0.44 \times f_u$ before the shank reached yielding.

Figure 38 through Figure 41, Figure 42 through Figure 45 and Figure 46 through Figure 48, shown under the next subsection headings, compare the experimental results to the analytical results (before yielding) from the calibrated models with $f_y = 70$ ksi and $f_u = 110$ ksi for the three specimens, respectively.

For all three models, the preload was applied by assigning a thermal expansion coefficient, and the temperature on the nut/washer element was continually increased until the strain at each gage location showed reasonable consistency with the experimental data. In general, the analytical results showed good agreement with the experimental results and the modeling approach appears valid for the parametric study, which is described in the next chapter.

Type-A Specimen Subject to Horizontal Loading

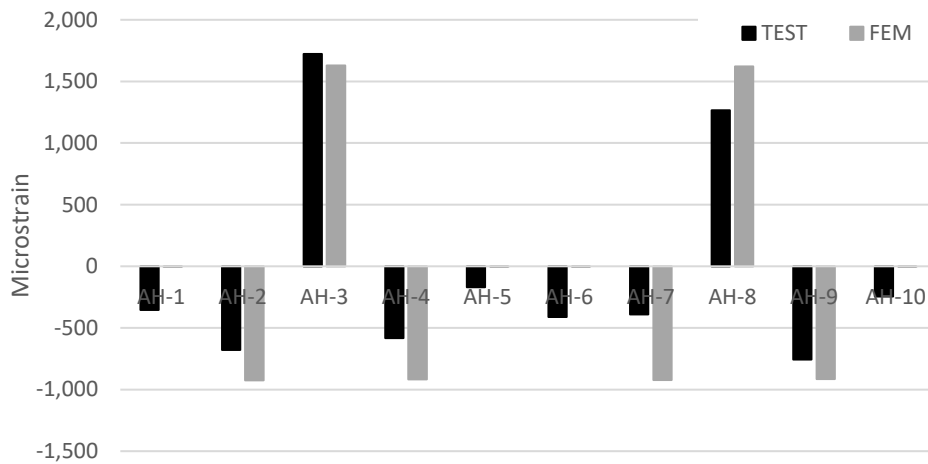


Figure 38. Model validation by U-bolt strain due to preload (Type-A, horizontal loading)

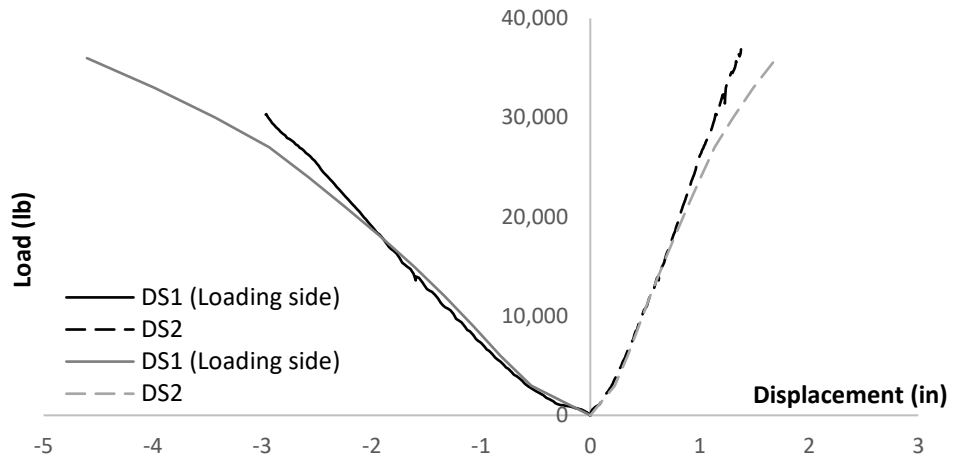
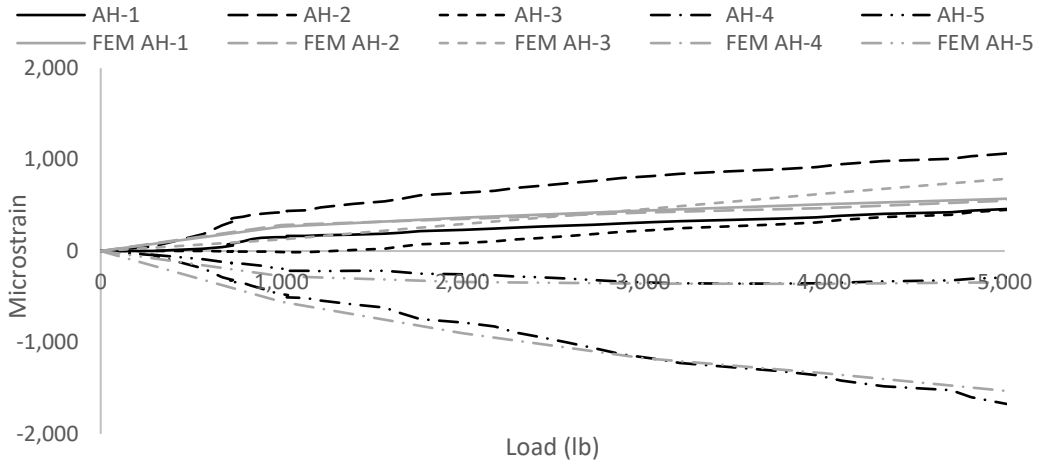
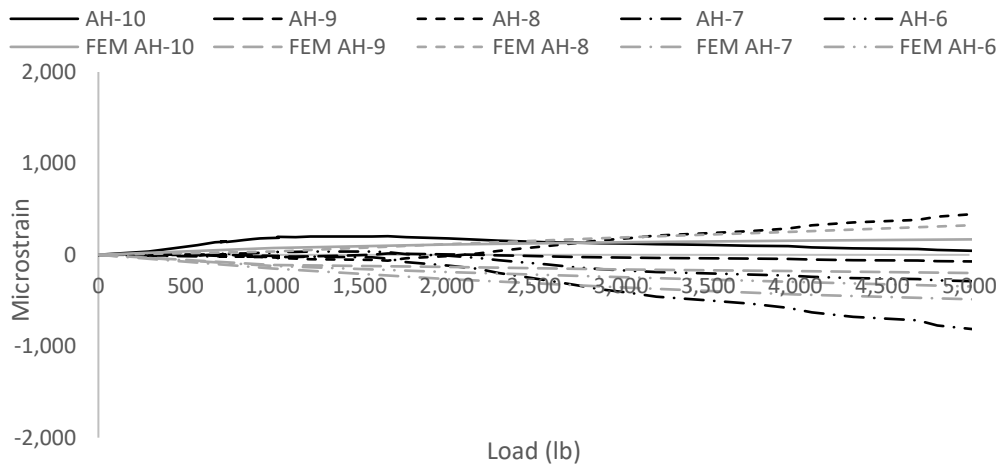


Figure 39. Model validation by load vs. displacement curves (Type-A, horizontal loading)



(a) Gage AH-1 to AH-5



(b) Gage AH-6 to AH-10

Figure 40. Model validation by U-bolt strain due to horizontal load (Type-A, horizontal loading)

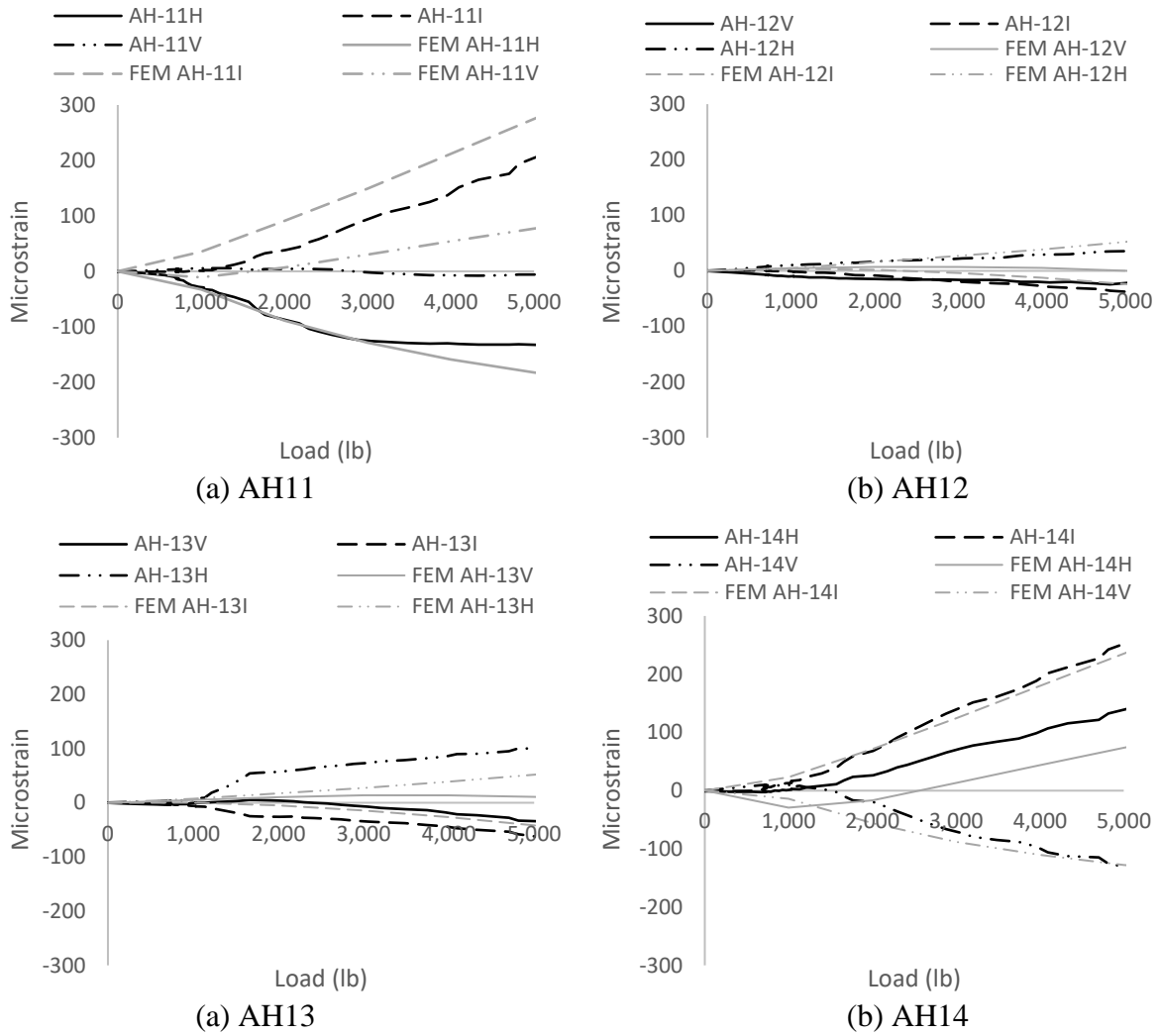


Figure 41. Model validation by strain from rosette strain gage (Type-A, horizontal loading)

Type-A Specimen Subject to Vertical Loading

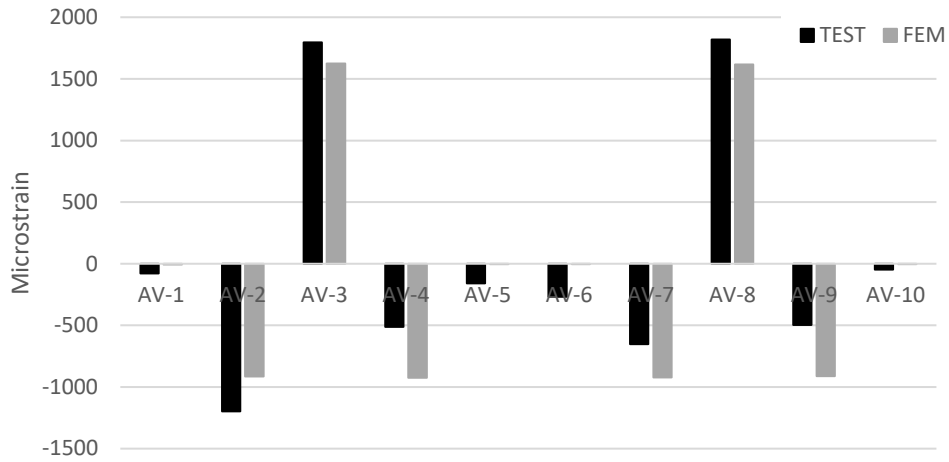


Figure 42. Model validation by U-bolt strain due to preload (Type-A, vertical loading)

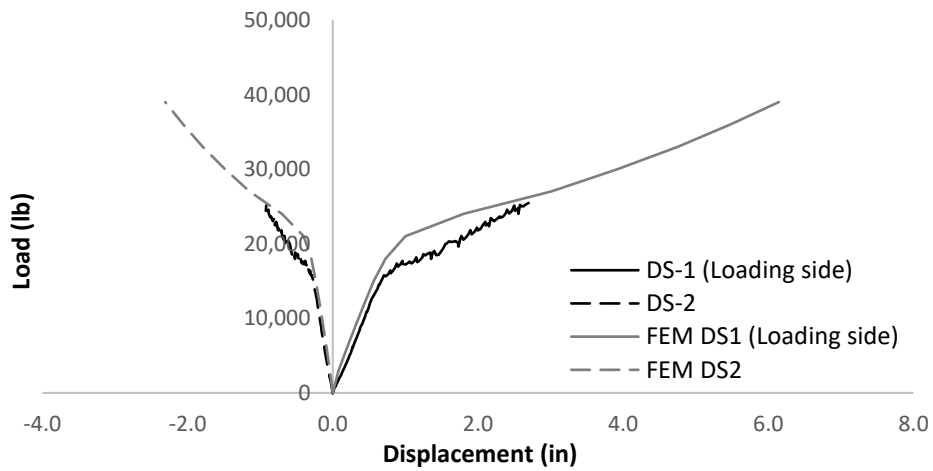
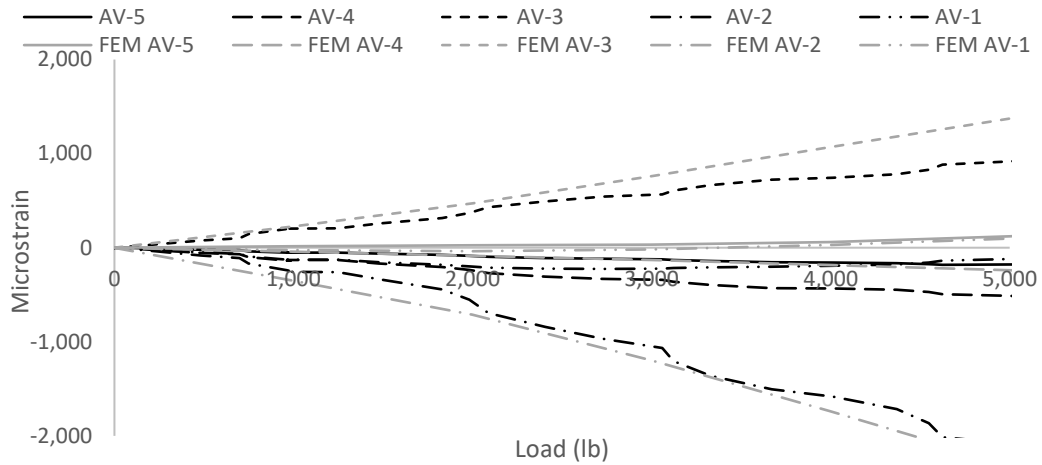
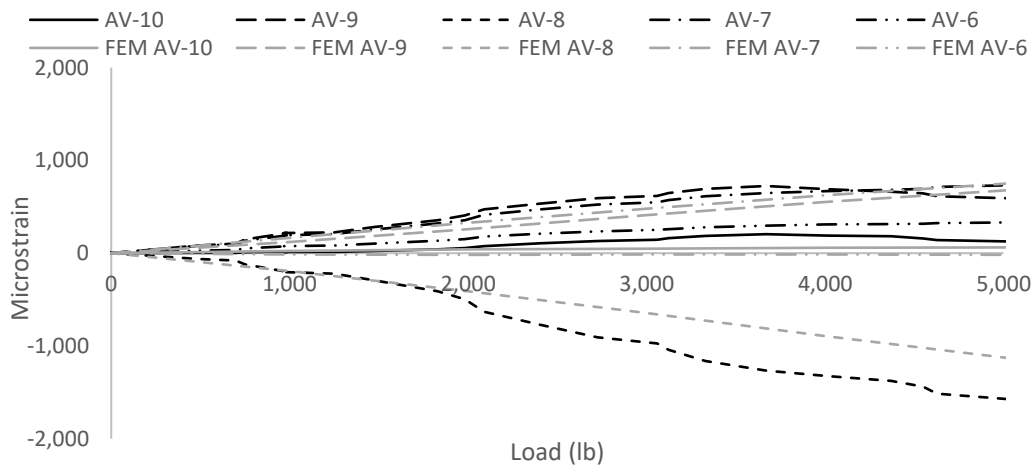


Figure 43. Model validation by load vs. displacement curves (Type-A, vertical loading)



(a) Gage AH-1 to AH-5



(b) Gage AH-6 to AH-10

Figure 44. Model validation by U-bolt strain due to vertical load (Type-A, vertical loading)

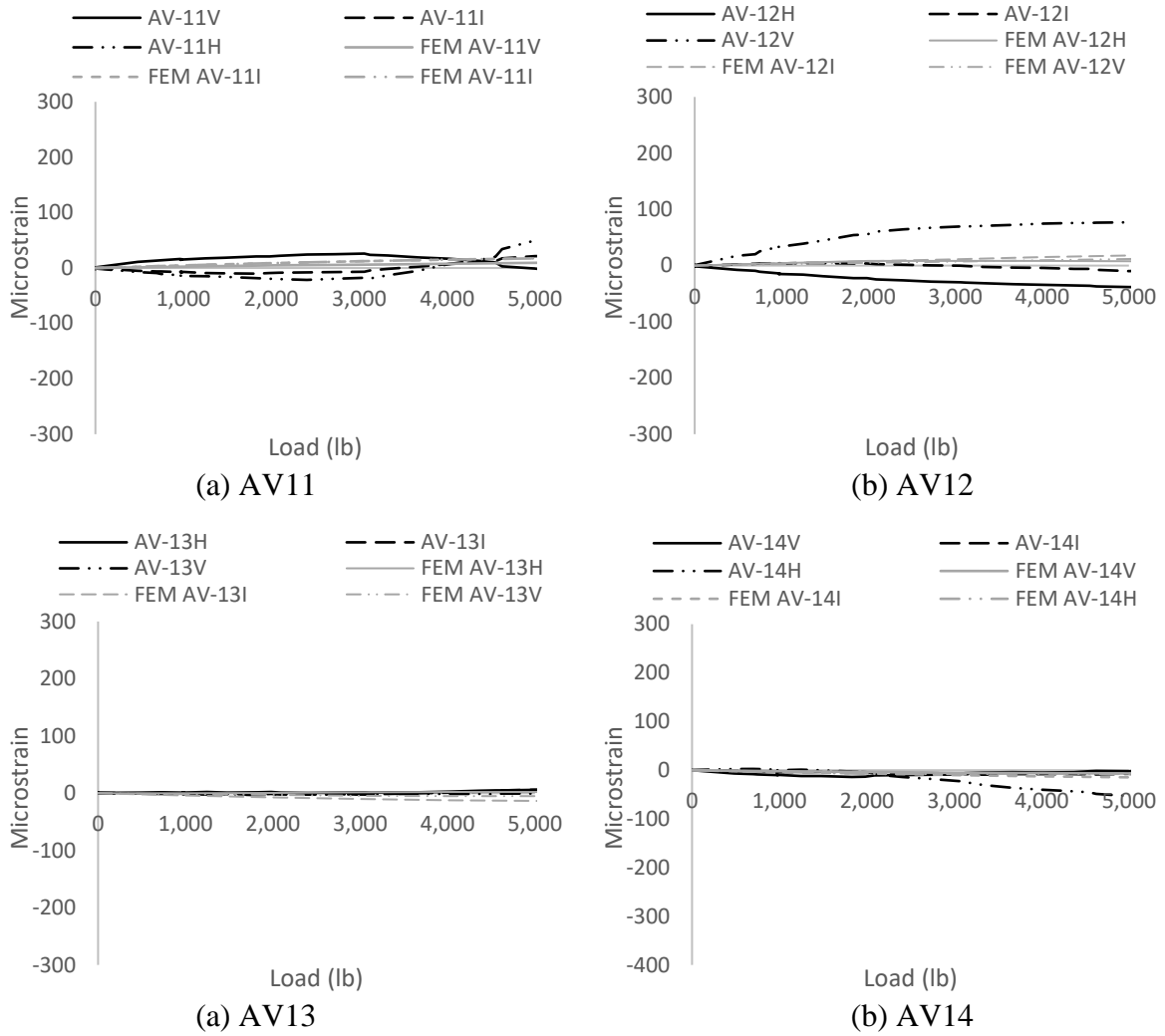


Figure 45. Model validation by strain from rosette strain gage (Type-A, vertical loading)

Type-B Specimen Subject to Horizontal Loading

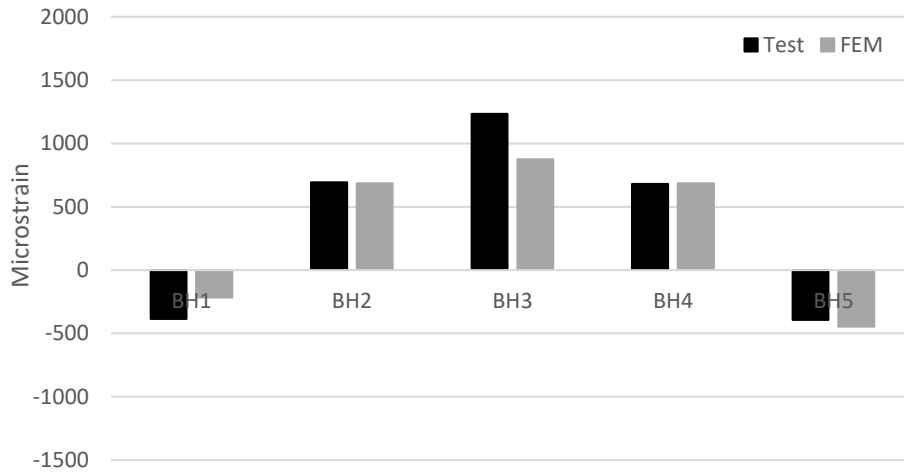


Figure 46. Model validation by U-bolt strain due to preload (Type-B, horizontal loading)

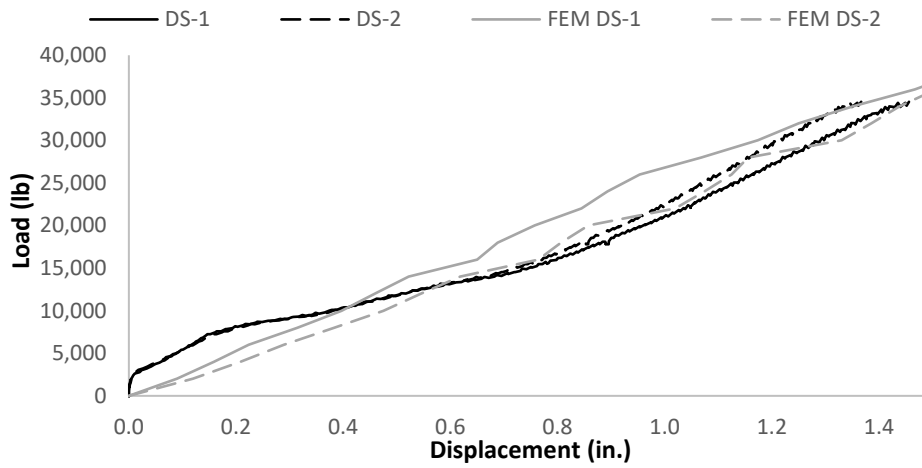


Figure 47. Model validation by load vs. displacement curves (Type-B, horizontal loading)

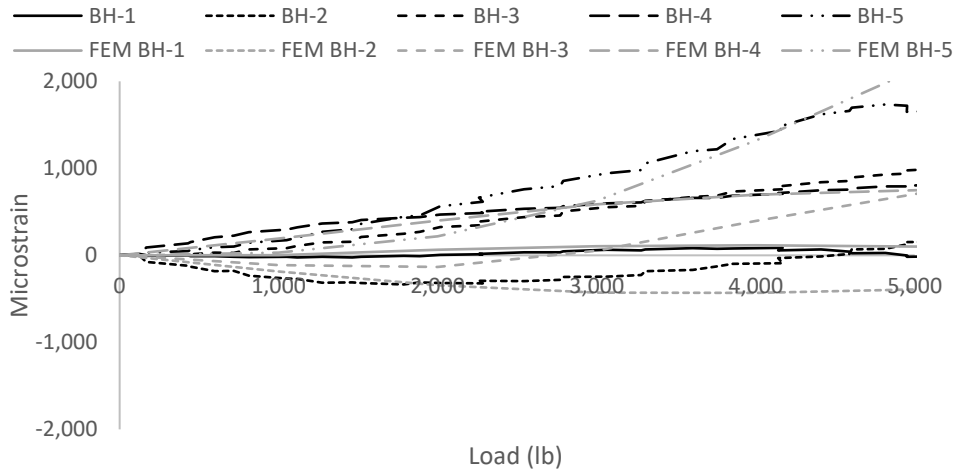


Figure 48. Model validation by U-bolt strain due to horizontal load (Type-B, horizontal loading)

CHAPTER 5. PARAMETRIC STUDY

The parametric study was performed to understand the behavior of the U-bolt connections with different material properties and subject to various loading conditions. Given that the laboratory tests on the specimens were conducted and the model calibration was performed based on the most frequently used 3/4-in. diameter U-bolt, the parametric study was also performed for the 3/4-in. diameter U-bolt connection.

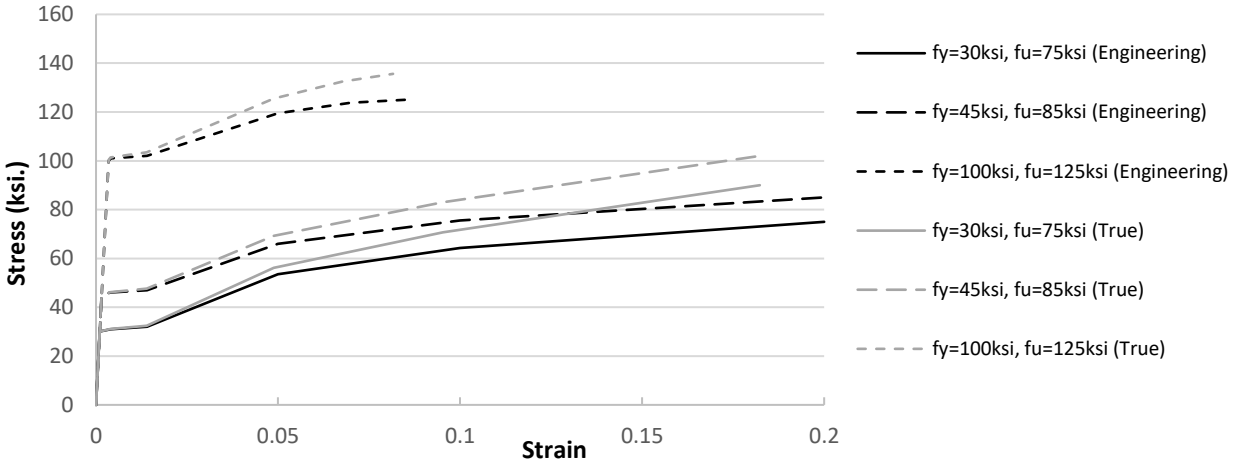
According to the Iowa DOT *Standard Specifications for Highway and Bridge Construction* Article 4187.01, C, 2 (with last revised 4/16/2019 at <https://www.iowadot.gov/erl/current/GS/content/4187.htm>), both galvanized steel U-bolts of various grades and stainless steel U-bolts of various grades are allowed for the U-bolt connections. Table 5 lists all of the types of steel that are allowed for the 3/4-in. diameter U-bolt.

Table 5. Materials of interest

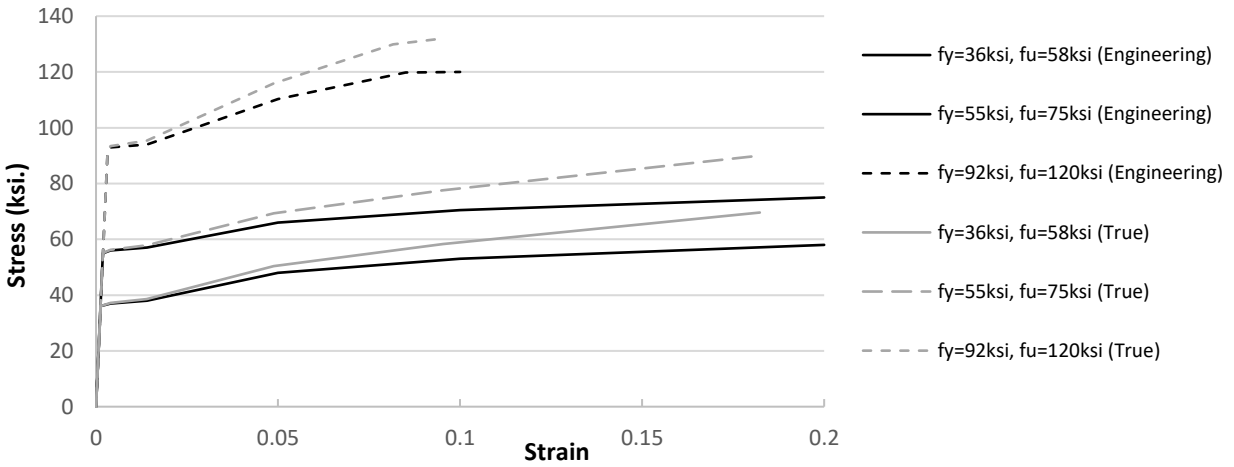
Steel Grade		Diameter (in.)	Yield Strength (ksi)	Ultimate Strength (ksi)	
Stainless Steel	ASTM A320, Class 1, Grade B8/B8A		All	30	75
	ASTM A320, Class 2, Grade B8		3/4 and under	100	125
	ASTM F593, Group 1, Alloy 304/304L	Condition A	1/4 to 1-1/2	30	75
		Condition CW2	3/4 to 1-1/2	45	85
	ASTM F593, Group 2, Alloy 316/316L	Condition A	1/4 to 1-1/2	30	75
		Condition CW2	3/4 to 1-1/2	45	85
	ASTM F593, Group 3, Alloy 321/347	Condition A	1/4 to 1-1/2	30	75
		Condition CW2	3/4 to 1-1/2	45	85
Galvanized Steel	ASTM A499, Type 1		1/2 to 1	92	120
	ASTM A307, Grade B		1/4 to 4	Not given	60
	ASTM F1554, Grade 36		1/4 to 4	36	58
	ASTM F1554, Grade 55		1/4 to 4	55	75

Initial Young's Modulus of 29,000 ksi for all

During the parametric study, all of the steel grades highlighted in yellow in Table 5 were studied. The ASTM A307, Grade B ($f_u = 60$ ksi) galvanized steel, whose yield strength is not defined, was not studied. The effects of these material properties were studied by modifying the constitutive models of the materials in the FEM, while the geometric properties of the FEM were kept the same. Figure 49 plots the stress-strain curves for the each type of material that was studied during the parametric study.



(a) Stainless steel



(b) Galvanized steel

Figure 49. Stress-strain curves of the materials studied during parametric study

The true stress-strain curve was converted based on the engineering stress-strain (shown in Figure 49), which was established with an initial Young’s modulus of 29,000 ksi and a peak strength strain of 0.2 ($f_u < 100$ ksi) and 0.1 ($f_u > 100$ ksi).

Additionally, the orientation of the loading relative to the beam was studied analytically to understand the behaviors of the specimens under those loading conditions. Figure 50 shows the loading directions relative to the vertical direction for the Type-A specimens.

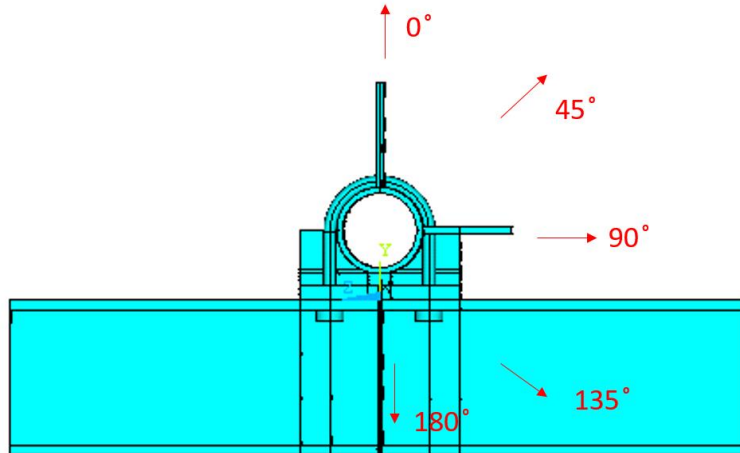


Figure 50. Parametric study loading directions relative to the vertical direction for the Type-A specimens

The Type-B specimen used the same method to designate the loading directions.

During the parametric study, one FEM was developed for each specimen type with a certain material property and loading direction, and analyzed with the nonlinear material and geometric properties. In total, 60 analyses were performed. Similar to the calibrated model, a preload was applied to the model until the U-bolt achieved a strain similar to that measured during testing. Then, the model was gradually loaded until failure occurred.

To gain an understanding of the structural behavior of both U-bolt connection types, both yield capacity and ultimate capacity results were output and are listed in Table 6.

Table 6. Parametric study results

Material Type		Stage of Interest		Type-A Specimen					Type-B Specimen				
				0°	45°	90°	135°	180°	0°	45°	90°	135°	180°
Stainless Steel	$f_y=30$ ksi $f_u=75$ ksi	Yield	Capacity (kips)	<1	<1	<1	<1	<1	8.5	1	1.5	1.5	3
			Location	Thread	Thread	Shank	Thread	Thread	Thread	Thread	Thread	Thread	Thread
		Ultimate	Capacity (kips)	18	15	24	19	23	41	12	29	17	14
			Location	Thread	Thread	Shank	Thread	Thread	Thread	Thread	Thread	Thread	Thread
	$f_y=45$ ksi $f_u=85$ ksi	Yield	Capacity (kips)	1	<1	1	<1	2	11.5	2	2.5	2	3
			Location	Thread	Thread	Shank	Thread	Thread	Thread	Thread	Thread	Thread	Thread
		Ultimate	Capacity (kips)	20	17	27	22	24	48	12	30	19	14
			Location	Thread	Thread	Shank	Thread	Pipe	Thread	Thread	Thread	Thread	Angle
	$f_y=100$ ksi $f_u=125$ ksi	Yield	Capacity (kips)	6	2.5	5.5	4	9	23	5	7	6.5	3
			Location	Thread	Thread	Shank	Thread	Thread	Thread	Thread	Thread	Thread	Thread
		Ultimate	Capacity (kips)	30	25	40	32	24	48	16	45	19	14
			Location	Thread	Thread	Shank	Pipe	Pipe	Thread	Thread	Thread	Thread	Angle
Galvanized Steel	$f_y=36$ ksi $f_u=58$ ksi	Yield	Capacity (kips)	1	<1	<1	<1	1	11	2	2	2	3
			Location	Thread	Thread	Shank	Thread	Thread	Thread	Thread	Thread	Thread	Thread
		Ultimate	Capacity (kips)	15	12	20	17	20	39	10	22	16	14
			Location	Thread	Thread	Shank	Thread	Thread	Thread	Thread	Thread	Thread	Thread
	$f_y=55$ ksi $f_u=75$ ksi	Yield	Capacity (kips)	3	1	2	1	3	14	2	4	3	3
			Location	Thread	Thread	Shank	Thread	Thread	Thread	Thread	Thread	Thread	Thread
		Ultimate	Capacity (kips)	19	15	25	21	24	44	12	29	19	14
			Location	Thread	Thread	Shank	Thread	Pipe	Thread	Thread	Thread	Thread	Angle
	$f_y=92$ ksi $f_u=120$ ksi	Yield	Capacity (kips)	5.5	2	4	3	8	21	4	6	5.5	3
			Location	Thread	Thread	Shank	Thread	Thread	Thread	Thread	Thread	Thread	Thread
		Ultimate	Capacity (kips)	28	24	39	32	24	48	16	42	19	14
			Location	Thread	Thread	Shank	Pipe	Pipe	Thread	Thread	Thread	Thread	Angle

To find the location that first achieved the yield or ultimate strain, small load steps were used in the analysis, and the results from each load step were carefully observed at the critical locations including U-bolt shank, thread, pipe, and angle. The yield or ultimate stage was identified when the strain at the critical location initially achieved the value corresponding to the yield or ultimate strength. Note that the yield or ultimate strengths at the thread region were reduced by a ratio of $0.31 \div 0.44$ to account for the thin cross-section at the thread region on the actual specimen.

The critical locations are shown previously in Figure 37-a and -b at the shank and thread for the Type-A model and in Figure 37-c at the thread for the Type-B model. Figure 51 and Figure 52 show the critical location (red) at the pipe and angle respectively.

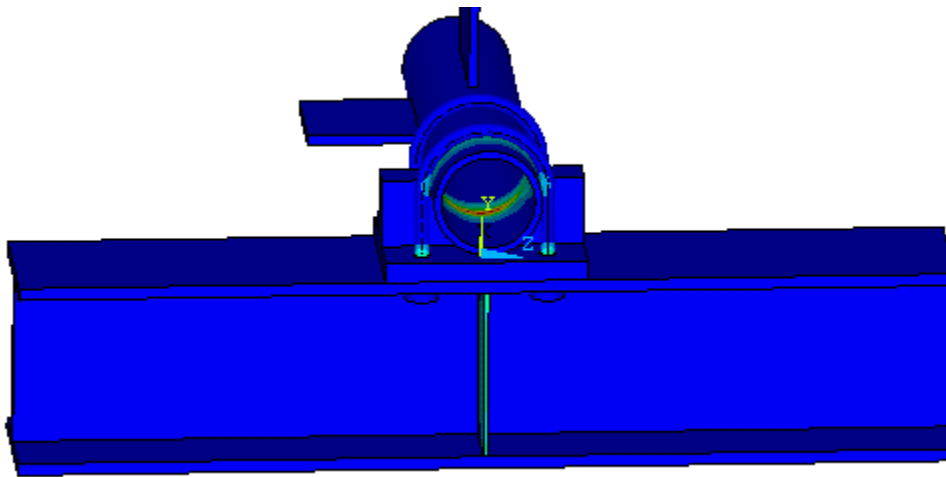


Figure 51. Critical location on pipe (Type-A)

TOEQV (AVG)
X =1.14278
X =.011281

ALCUTEMIL
FEB 12 2019
09:41:37

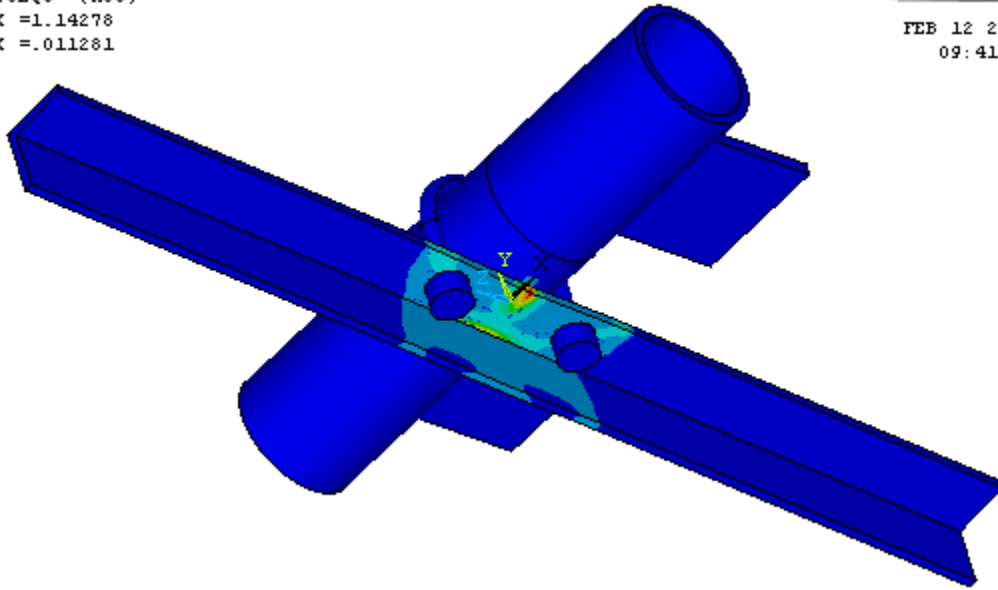


Figure 52. Critical location at the angle (Type-B)

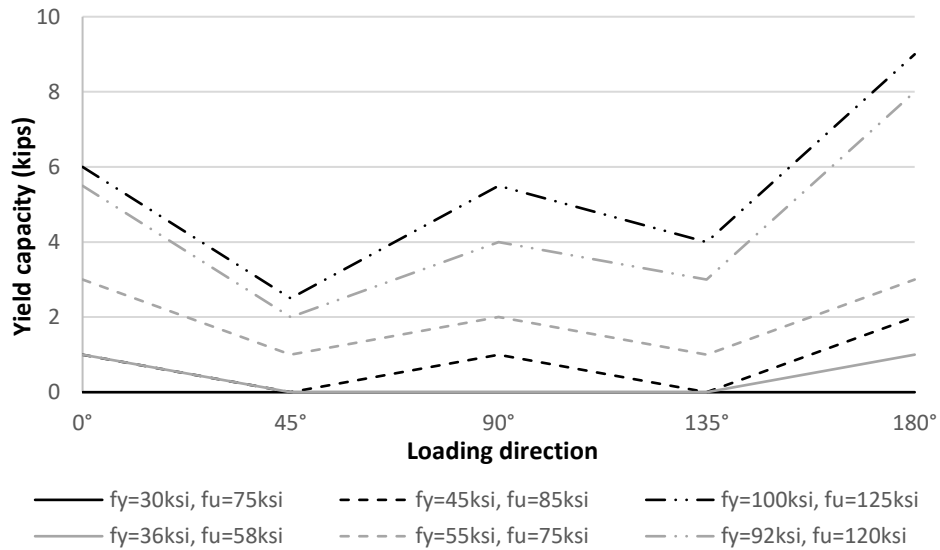
Note that, for the Type-B model subject to 180° loading, the load was carried by the angle without inducing any stress on the U-bolt.

The results shown previously in Table 6 show a relatively low yield capacity but high ultimate capacity, which indicates a good ductility before reaching failure. It also could be concluded that the thread region is the most vulnerable location, as most of the failures start in that region.

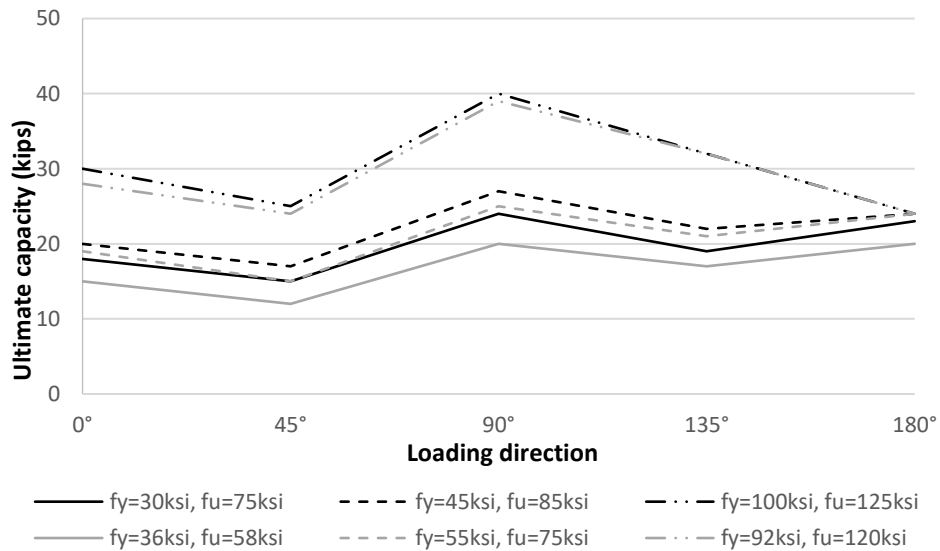
Interaction diagrams were created based on these data, as discussed in the next chapter.

CHAPTER 6. INTERACTION DIAGRAMS

The interaction diagrams shown in Figure 53 and Figure 54 were developed based on the results from the parametric study (previous Table 6).

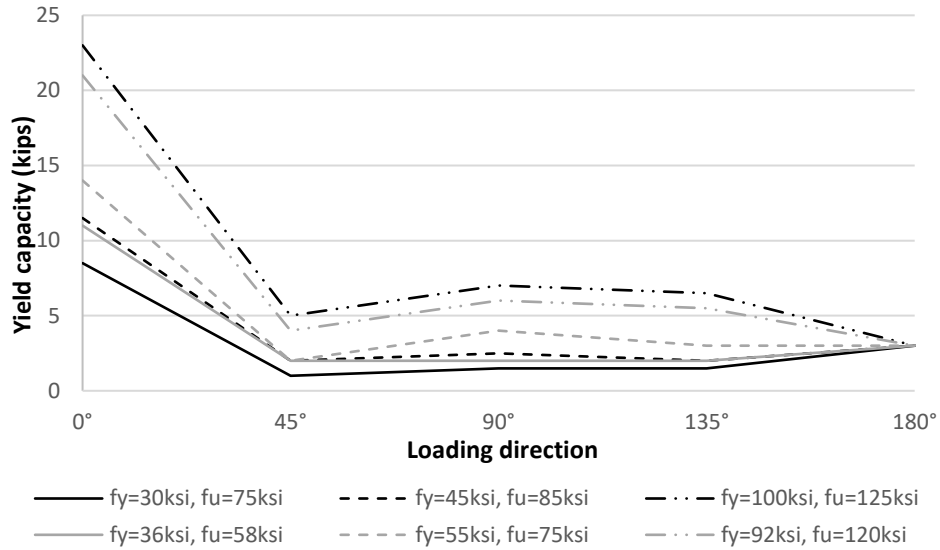


(a) Yield capacity of Type-A specimen

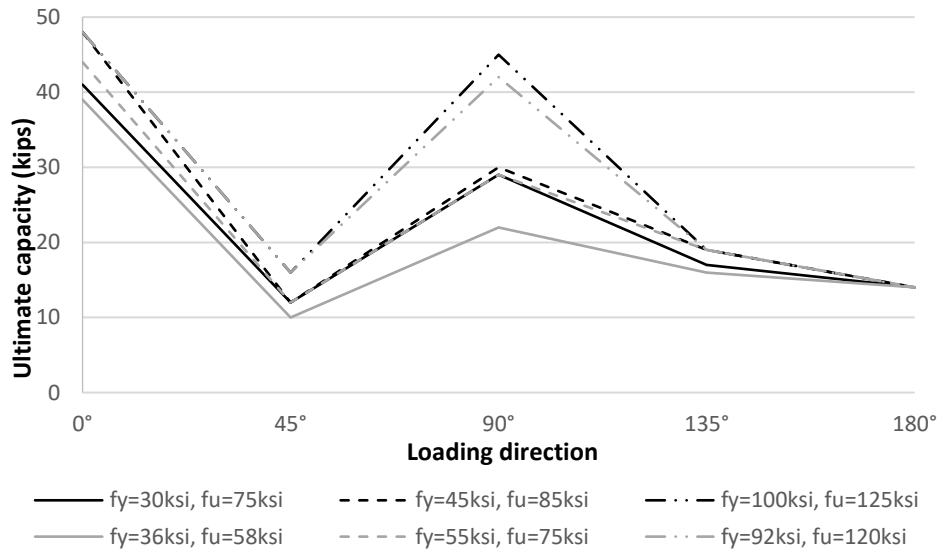


(b) Ultimate capacity of Type-A specimen

Figure 53. Interaction diagram for Type-A specimen



(a) Yield capacity of Type-B specimen



(b) Ultimate capacity of Type-B specimen

Figure 54. Interaction diagram for Type-B specimen

The interaction diagrams were created for the estimation of the capacity of the U-bolt connections under different loading conditions without the need to conduct any load testing or numerical simulations. By using Figure 53 and Figure 54, a designer can easily find the capacities by inputting the material type and load resultant direction. To use the interaction diagrams in this chapter, the following limitations should be considered:

- The capacities presented in the interaction diagrams are only for the 3/4-in. diameter U-bolt on the specific connection structure (Type-A or Type-B).

- The laboratory tests were performed with loading directions of only 0° and 90° for Type-A specimens and 90° for the Type-B specimen. The results for other loading directions were obtained from the analytical study.
- The capacities for the loading directions with exceptions of 0° , 45° , 90° , 135° , and 180° were interpolated from the analytical results at those five loading directions. The actual capacities may vary.
- The capacities were calculated on a system basis, not just the U-bolt. For example, under certain conditions, the Type-B system first yielded or achieved the ultimate strength on the pipe or angle, not the U-bolt. The replacement of accessory parts, such as the angle or pipe, may change the system capacity.

CHAPTER 7. SUMMARY, CONCLUSIONS AND FUTURE RESEARCH DIRECTIONS

7.1 Summary

A comprehensive literature search on the utilization of and modeling of U-bolt connections was conducted for this research project. Three laboratory tests were conducted on two types of specimens. The data collected from the tests were analyzed and then used to calibrate various FEMs. The calibrated models were then used in the parametric study to calculate the yield and ultimate capacities of both specimen types with various material properties and load directions. Finally, interaction diagrams were developed for capacity estimation the of the U-bolt connections.

7.2 Conclusions

A few conclusions can be summarized from different phases of this work as follows:

- Not many research investigations on the capacity of U-bolt connection have been conducted in the field of civil engineering. In addition, most manufacturers of U-bolts do not intend for them to be used in the ways currently detailed.
- The results from both laboratory tests and analytical solutions indicate that different failure modes occur when the loading is in different directions.
- The results from the analytical study show a relatively low yield capacity, but indicate that the details have good ductility before reaching failure.
- The parametric study results indicate that the thread region is the most vulnerable location and that most of the failures start from that region.

7.3 Future Research Directions

The research summarized in this report represents a major step toward developing a better understanding of the behavior and design of U-bolt connections. However, several questions remain that could be answered by conducting additional research, as follows:

- Additional laboratory tests should be performed on high-strength U-bolts with loading directions of 135° and 180° , because the failure locations predicted by the FEM analyses with high-strength U-bolts are different from those captured in the laboratory tests.
- More experimental and analytical work should be conducted with various loading directions (e.g., 30° , 60° , 120° , and 150°) to study structural behavior subject to various loading directions.

- Given that almost all of the material types appear to have low yield capacity, the fatigue performance of the U-bolt connection should be investigated to understand the impact of repeated loads near the yield load. Additional laboratory tests are recommended to study the fatigue performance of the U-bolt connections.
- Given that both experimental and analytical work were conducted on the 3/4-in. diameter U-bolt, further research is recommended on U-bolt connections with other sizes to obtain the relationship between the U-bolt size and connection capacity.

REFERENCES

- Diamantoudis, A. T. and C. A. Apostolopoulos. 2002. Body Mounting and ADR Requirement for Tank Vehicles Carrying Dangerous Goods, *Technical Chronicle of Science Journal*, Vol. 4, No. 1–2, in Greek with extended summary in English, pp. 19–27.
- Ju, S.-H., C.-Y. Fan, and G. H. Wu. 2004. Three-Dimensional Finite Elements of Steel Bolted Connections. *Engineering Structures*, Vol. 26, No. 3, pp. 403–413.
- Kim, J., J.-C. Yoon, and B.-S. Kang. 2007. Finite Element Analysis and Modeling of Structure with Bolted Joints. *Applied Mathematical Modelling*, Vol. 31, No. 5, pp. 895–911.
- Kirby, D. and R. Charniga. 2005. *A Finite Element and Experimental Analysis of a Light Truck Leaf Spring System Subjected to Pre-Tension and Twist Loads*. Technical Paper No. 2005-01-3568. 2005 SAE Commercial Vehicle Engineering Conference, November, Chicago, IL.
- McCarthy, C. T. and M. A. McCarthy. 2005. Three-Dimensional Finite Element Analysis of Single-Bolt, Single-Lap Composite Bolted Joints: Part II—Effects of Bolt-Hole Clearance. *Composite Structures*, Vol. 71, No. 2, pp. 159–175.
- McCarthy, M. A., C. T. McCarthy, V. P. Lawlor, and W. F. Stanley. 2005. Three-Dimensional Finite Element Analysis of Single-Bolt, Single-Lap Composite Bolted Joints: Part I—Model Development and Validation. *Composite Structures*, Vol. 71, No. 2, pp. 140–158.
- Shetty, M. K. 2006. Development of a Lead Spring U-Bolt Load Transducer: Part of an Onboard Weighing System for Off-Highway Log Trucks. MS thesis. University of British Columbia, Vancouver.